



## APPROVAL SHEET

Title of Dissertation: Measuring Early Pre-symptomatic Changes in Locomotion of Rodent Models of Neurological and Neuromuscular Diseases

Name of Candidate: Wenlong Tang  
Doctor of Philosophy, 2010

Dissertation and Abstract Approved: \_\_\_\_\_  
Dr. Uri Tasch  
Professor  
Department of Mechanical Engineering  
University of Maryland, Baltimore County

Date Approved: \_\_\_\_\_

## Curriculum Vitae

**Name:** Wenlong Tang.

Degree and date to be conferred: Ph.D., 2010

Place of Birth: Liaoyuan, Jilin, China.

Secondary education: Beijing University of Technology, Beijing, China, 2007.

### Collegiate institutions attended:

- **Ph.D.**, Mechanical Engineering, **01/2007-11/2010**, University of Maryland, Baltimore County.
- **M.S.**, Mechanical Engineering and Applied Electronic Technology, **09/2004-12/2006**, Beijing University of Technology.
- **B.S.** Mechanical Engineering and Automation, **09/2000-07/2004**, Beijing University of Aeronautic and Astronautic.

### Professional Publications:

#### Journal Publications

- 1) **Tang, W.**, Tasch, U., Neerchal, N. K., Zhu, L. Yarowsky, P., *Measuring early pre-symptomatic changes in locomotion of SOD1-G93A rats – a rodent model of Amyotrophic Lateral Sclerosis*, J. of Neurosci. Methods, 2009; 176(2): 254-262.
- 2) **Tang, W.**, Lovering, M. R., Roche, A. J., Bloch, J. R., Neerchal, N. K., Tasch, U., *Gait analysis of locomotory impairment in rats before and after neuromuscular injury*, J. of Neurosci. Methods, 2009; 181(2): 249-256.
- 3) **Tang, W.**, McDowell, K., Limsam, M., Yarowsky, P., Tasch, U., *Locomotion analysis of Sprague-Dawley rats before and after injecting 6-OHDA*. Behavioral Brain Research, 2010; 210:131-133.
- 4) **Tang, W.**, Tasch, U., *Detecting ALS and Parkinson ' s disease in rats through locomotion analysis*. Neurology Research International, 2010; under review.
- 5) Feng, X., **Tang, W.**, Tasch, U., Neerchal, N., *Designing a Study for Developing Predictive Models for Gait Abnormality in Rat*. J. of Statistical Computation and Simulation, under review.

## Conferences

- 6) **Tang, W.**, McDowell, K., Limsam, M., Yarowsky, P., Tasch, U., *Early detection of gait abnormalities in Sprague-Dawley rats after injection of 6-hydroxydopamine*. The 3rd International Congress on Gait & Mental Function. Feb. 26-28. Washington D.C., USA, 2010.
- 7) **Tang, W.**, Lovering, R. M., Roche, J. A., Neerchal, N. K., Tasch, U., *Gait analysis of locomotory impairment in rats before and after neuromuscular injury*. Society for Neurosci. Annual Conference. Oct. 17–21. Chicago, IL, USA, 2009.
- 8) Tasch, U., Moubarak, P., **Tang, W.**, Zhu, L., Lovering, R. M., Roche, J. A., Bloch, R. J., *An instrument that simultaneously measures spatial gait parameters and ground reaction forces of locomoting rats*. Proceedings of the 9th Biennial ASME Conference on Engineering Systems Design and Analysis. ESDA08. July 7-9. Haifa, Israel, 2008.
- 9) **Tang, W.**, Zhang, W., *Studies on the Dynamics and Control Theory of Inverted Pendulum on Feedback Control*, the 2nd International Conference in Dynamics, Vibration and Control. ICDVC-2006. August 23-26. Beijing, China, 2006.

## ABSTRACT

Title of Document: Measuring Early Pre-symptomatic Changes in Locomotion of Rodent Models of Neurological and Neuromuscular Diseases

Wenlong Tang, Doctor of Philosophy, 2010

Directed By: Dr. Uri Tasch  
Professor  
Department of Mechanical Engineering  
University of Maryland, Baltimore County

Neurological and neuromuscular diseases are usually difficult to diagnose at early stages. The aim of this Ph.D. dissertation is to detect neurological and neuromuscular diseases early by using a gait analysis system in laboratory rats. This includes diseases such as Amyotrophic Lateral Sclerosis, muscular injuries, and Parkinson's disease. Several preliminary experiments have been developed on rodents that have been used as animal models for human diseases. This work developed an effective noninvasive diagnostic methodology which can provide the probability that a rat is exposed to a disease that affects its locomotion. The gait analysis system measures ground reaction forces and associated time and frequency parameters when a rat walks on the sensor module. These measurements are used as input to a logistic regression model that assesses the probability that the animal model has a specific disease that affects its locomotion.

All the models we have developed have achieved specificity and sensitivity values of at least 90%. This dissertation has the potential to have a significant impact on helping to diagnose diseases that affect locomotion early, which is currently very difficult to do effectively. This new methodology also has the potential to be instrumental in finding and validating new therapeutic procedures for the studied ailments.

MEASURING EARLY PRE-SYMPTOMATIC CHANGES IN LOCOMOTION  
OF RODENT MODELS OF NEUROLOGICAL AND NEUROMUSCULAR  
DISEASES

By

Wenlong Tang

Dissertation submitted to the Faculty of the Graduate School of the  
University of Maryland, Baltimore County, in partial fulfillment  
of the requirements for the degree of  
Doctor of Philosophy  
2010

UMI Number: 3439760

All rights reserved

INFORMATION TO ALL USERS

The quality of this reproduction is dependent upon the quality of the copy submitted.

In the unlikely event that the author did not send a complete manuscript and there are missing pages, these will be noted. Also, if material had to be removed, a note will indicate the deletion.



UMI 3439760

Copyright 2011 by ProQuest LLC.

All rights reserved. This edition of the work is protected against unauthorized copying under Title 17, United States Code.



ProQuest LLC  
789 East Eisenhower Parkway  
P.O. Box 1346  
Ann Arbor, MI 48106-1346



© Copyright by  
Wenlong Tang  
2010



## Dedication

To my grandmother, here is what your favorite grandson did when they are absent.

## Acknowledgements

I have been fortunate to be associated with a number of individuals who have guided me through this research.

I would first like to express sincere appreciation to the committee chair, my academic advisor, Dr. Uri Tasch for his invaluable excellent guidance, support and patience throughout the course of this research. His versatility and broad knowledge are something I will benefit from and will help me in my future life.

In addition, to the members of the advisory committee, Dr. Richard M. Lovering, Dr. Nagaraj Neerchal, Dr. Liang Zhu and Dr. Marc Zupan are greatly acknowledged for their time, advice and encouragement. Thanks are also due to Dr. L. D. Timmie Topoleski, the graduate program director in the department of mechanical engineering at UMBC, who kindly provided a lot help during my whole graduate study.

Special thanks are due to Dr. Richard M. Lovering and Dr. Paul Yarowsky from University of Maryland, School of Medicine, who provide the surgeries and injections of the animals, and valuable discussions through the whole research progress.

This research would not have been possible without the constant support of my parents, my wife Di, and my lab mates, Dr. Priya Narayanan, Dr. Jianbo Liu, Mr. Philip Dyer, Mr. Paul Moubarak, Mr. Michael Biskach and Mr. Payam Motabar. Their belief in me was very encouraging and it inspired my work at all times. I am indeed blessed to have such caring and supportive family and friends.

Finally, all the best wishes are given to all members in the Department of Mechanical Engineering in UMBC!

## Table of Contents

Dedication.....	I
Acknowledgements.....	II
Table of Contents.....	IV
List of Tables.....	VI
List of Figures.....	VII
Chapter 1: Introduction.....	1
1.1 Background.....	1
1.2 Objectives and Specific Aims.....	11
1.3 Dissertation Overview.....	12
Chapter 2: Methodology.....	13
2.1 Gait Analysis System.....	13
2.2 Locomotion Parameters (LPs).....	18
2.3 Logistic Regression Model.....	21
2.4 Animal Protocols.....	21
Chapter 3: Measuring Early Pre-symptomatic Changes in Locomotion of Rodent Models of SOD1-G93A- a Rodent Model of Amyotrophic Lateral Sclerosis.....	23
3.1 Introduction to the Rodent ALS Models.....	23
3.2 Materials and Methods.....	25
3.2.1 Obtaining Gait Measurements for the ALS Experiment.....	25
3.2.2 Logistic Regression.....	26
3.2.3 Cross Validation.....	26
3.3 Results of the ALS Experiment.....	27
3.4 Discussion of the ALS Experiment.....	35
Chapter 4: Gait Analysis of Locomotory Impairment in Rats Before and After Neuromuscular Injury.....	37
4.1 Introduction to the Locomotory Impairment.....	37
4.2 Methods and Materials.....	39
4.2.1 Associating Segments of Load cell Signals and Limbs.....	39
4.2.2 Obtain Gait Measurements for the Locomotory Impairment Experiment.....	41
4.2.3 Assessing the Severity of Locomotory Impairment.....	42
4.3 Results of the Locomotory Experiment.....	42
4.4 Discussion of the Locomotory Experiment.....	48
Chapter 5: Locomotion Analysis of Sprague-Dawley Rats Before and After Injecting 6-OHDA.....	50
5.1 Introduction to the Parkinsonian Models.....	50
5.2 Methods and Materials.....	52
5.2.1 Animal Experiment and Surgery.....	52
5.2.2 Obtain Gait Measurements for the Parkinsonian Experiment.....	53
5.2.3 Cross Validation of Logistic Regression Model.....	54
5.3 Results of the Parkinsonian Experiment.....	54
5.4 Discussion of the Parkinsonian Experiment.....	57
Chapter 6: Conclusion and Future Work.....	59

6.1 Conclusion .....	59
6.2 Future Work .....	61
6.2.1 Improving the Models by Running Larger Sample Sizes .....	61
6.2.2 Application of the Methodology to Human .....	63
Appendix: Designing a Study for Developing Predictive Models for Gait Abnormality in Rats .....	64
Bibliography .....	75

## List of Tables

Table 1.1 Description of gait parameters that were used to evaluate change in gait following intraarticular injection of carrageenan by DigiGait™ (Berryman <i>et al.</i> , 2009).....	8
Table 1.2 Description of gait parameters that were used to evaluate change in gait by CatWalk™ (Neumann <i>et al.</i> , 2009; Deumens <i>et al.</i> , 2007).....	10
Table 2.1 Definitions of the 20 LPs evaluated in this dissertation.....	19
Table 3.1 Definitions of 15 symmetry factors.....	29
Table 3.2 Numerical values of the 20 measured LPs for each (LF, RF, LH, RH) limbs and the 15 symmetry factors for fore and hind limbs for a control rat #107.....	30
Table 3.3 Misclassification rate, in percentage, obtained by using a single LP or its associated transform TLP.....	32
Table 4.1 Numerical values of the 20 measured LPs for a permanently impaired and control rats. Data of the permanently impaired rat were recorded when the denervated rat was 114 days old and 12 days after introducing the permanent locomotory impairment. Data of the control rat, recorded at 94 days of age. Note the generally reduced force capacity of the LH limb of the denervated rat. Except for stance time, $F_z$ and $F_y$ , all other variables are non dimensional.....	44
Table 4.2 Ranking the transformed LPs based on their misclassification performance when a single TLP is used at a time. The misclassification rate of the Fourier transform of the vertical reaction force, $F_z\omega$ , is the best with misclassification rate of 26.5%, and the time duration during which the longitudinal reaction is propelling, NP, has the worst performance with misclassification rate of 28.8%.....	45
Table 5.1 The seven LPs that best distinguish the locomotion of 6-OHDA from controls, along with their definitions and misclassification rates.....	53
Table 5.2 The LPs that best distinguish between the locomotion of rat models of ALS, Parkinson and muscular injury. Note that different sets of LPs are required for distinguishing SOD1-G93A, 6-OHDA, and injured rats from their corresponding controls. ....	56



## List of Figures

- Figure 1.1** Muscle Injury Model: the tibia of the hindlimb was stabilized and the foot secured to a plate driven by a stepper motor. The peroneal nerve was used to stimulate the TA anterior (a dorsiflexor) at a selected time while the plate forced the foot into plantar flexion at a selected velocity (Lovering *et al.*, 2005).....5
- Figure 1.2** Miniature force platform. Semiconductor strain gauges mounted on spring blades are sensitive to vertical and horizontal deformation of the beams caused by forces exerted when the animal moves over the wooden cover (Full and Tu, 1990)...6
- Figure 1.3 (a)** By measuring the ground reaction forces in vertical direction, it was found that the mass center of a control rat followed a sine wave when the rat was walking while Parkinson's rats didn't (Muir and Whishaw, 1999).....6
- Figure 1.3 (b)** By measuring the ground reaction forces in vertical direction, it was found that the sum of the forces from diagonal legs during about the same period of time has only one peak for control rats while the rats with Parkinson's disease have more than one peaks (Muir and Whishaw, 1999).....7
- Figure 1.4** DigiGait™ made by Mouse Specifics Inc. The system has a treadmill on the bottom of the transparent compartment. The speed of the treadmill and the size of the compartment are adjustable. A video camera records bottom images of the rat that walks through the system. All the locomotion parameters are generated from the analysis of the images.....8
- Figure 1.5** CatWalk™ invented by Noldus Information Technology. The floor of the system is transparent and lightened by arrays of LED. Only at the points where a paw touches the glass, light exits the floor and scatters at the paw, illuminating the points of contact only (Noldus IT, 2006).....9
- Figure 2.1** A gait analysis system for rodents. The system measures *LPs* in 4 domains: force, space, time, and frequency. The measured forces are in vertical, longitudinal, and transverse directions. A video camera records bottom images of the rat that walks through the system, and through synchronization of the video images and load cell signals, one can recognize the ground reaction forces of each individual limb.....14
- Figure 2.2** The new version of data collection software for gait analysis system programming by LabVIEW®. Forces data and the video data start to be collected at the same time when the data collection software is run. As soon as the software is stopped, there will be two files created in a specific folder automatically, which store force data and video images.....15
- Figure 2.3** A typical output generated by the GAS from a typical test run. The signatures of the left and right limbs are depicted on the left and right sides. The transverse ( $F_x$ ), longitudinal ( $F_y$ ), and vertical ( $F_z$ ) are normalized with respect to the rat's body weight and plotted as a function of time ( $s$ ). The longitudinal ( $Y$ ) and transverse ( $X$ ) limb positions are normalized with respect to the length and width of the floor plates, respectively. A video image of the bottom of the rat is also recorded.....16
- Figure 2.4** To associate a load-cell signature with a limb, the computer mouse is placed on a selected signature (vertical marker); and the most recent video image is

displayed. The load-cell signature on the right from 0.36 to 5.0 s is associated with the right fore limb.....	17
<b>Figure 2.5</b> The load signatures generated by a single limb are identified and following the procedure shown in Figure 2.4, the fore and hind limbs are marked with dashed and solid heavy lines, respectively.....	18
<b>Figure 3.1</b> The range of predicting probabilities that the examined rat belongs to the SOD1-G93A group. Note large spread and big overlap between the control and SOD1-G93A groups when 1 Variable is used. When 4 Variables are used the overlap between the two groups shrinks a little, nevertheless when a 7-variable model is used there is an almost complete separation between the control and the SOD1 groups. This separation enables us to classify the rats correctly in each and every test run....	33
<b>Figure 3.2</b> Probability of ALS for 4 SOD1 and 4 control rats vs. days for the animals that traversed through the noninvasive diagnostic system. Note that P (ALS) for SOD1 and control rats are close to 1.0 and 0.0, respectively, in all days except for a single day for rat #4.....	34
<b>Figure 4.1</b> A schematic of the gait analysis system for rodents. The system measures locomotion parameters in 4 domains: force, space, time and frequency. The measured forces are in vertical (Z), longitudinal (Y) and transverse (X) directions. The locomotion parameters feed a statistical model that calculates the probability that a rodent displays locomotion impairment.....	38
<b>Figure 4.2</b> To associate load cell signatures with a limb the computer mouse is placed on a selected signature (vertical red marker) and the most recent video image is displayed. The load cell signature on the right floor-plate from 0.63 to 0.79 s is associated with the right fore limb. ....	39
<b>Figure 4.3</b> The load signatures generated by a single limb are identified and the fore and hind limbs are marked with dashed and solid heavy lines, respectively.....	40
<b>Figure 4.4</b> The range of predicting probabilities that the examined rat has locomotory impairment when 1, 2, 3, . . . and , 6 top performing <i>TLPs</i> (listed in Table 4.2) are used. C is control and D is denervated or permanently impaired groups. The cutoff value of the probability predictions for the control and denervated groups was 0.5. Note the improved specificity and sensitivity of the control (C) and denervated (D) groups, as the number of <i>TLPs</i> increases from 1 to 6. ....	46
<b>Figure 4.5</b> The probability of locomotory impairment of the three injured rats. Large strain injury was induced on day 0. The alteration in gait after injury is reflected by the high probability of locomotion impairment at day 0. Despite, animal to animal variability in gait during the 5 weeks after injury, the probability of locomotion impairment for all three animals returned to pre-injury levels by the 34th day. The cutoff value of the probability predictions for locomotory impairment was 0.5. The vertical bars are the error bars.....	47
<b>Figure 5.1</b> Sensitivity and specificity versus the number of best performing locomotion parameters ( <i>LPs</i> ) used to model the locomotion of the 6-OHDA lesioned rats. Best performing <i>LPs</i> result in the lowest misclassification errors when the cutoff value is set to 0.5. Note the improved specificity and sensitivity values (0.84–0.95 and 0.63–0.92, respectively) as the number of best performing <i>LPs</i> increases from 1 to 7.....	55
<b>Figure 5.2</b> The probability that a rat is parkinsonian for the six rats, 10 days prior to	

and 20 days post-operation. Each data point is an average of minimum two predictions, calculated by the 7-LP model based on leave-one-out method. Note the maximum probability value prior to the 6-OHDA lesion is 0.34, and the minimum probability value after the operation is 0.67. ....56

**Figure 6.1** Classification rate versus the number of rats per group for the SOD1-G93A experiment. Vertical lines represent the standard deviation of classification rate.....62

**Figure 6.2** Maximum standard deviation of the coefficients of the logistic regression models for SOD1-G93A laboratory rats. ....63

## Chapter 1: Introduction

### 1.1 Background

Recently, increasing number of people affected by neurodegenerative diseases such as Amyotrophic Lateral Sclerosis (ALS), neuromuscular injuries, and Parkinson's disease (PD) create a growing need for effective diagnosis and treatment protocols (Liao *et al.*, 2008). An estimated 6.8 million people die every year as a result of neurological disorders all over the world and 127 million Europeans currently suffer from one or more neurological disorders. An American study estimated the cost of multiple sclerosis in 2004 in the US was 8.3 billion dollars. In Europe, the economic cost of direct medical expenditures for neurological diseases alone was estimated at about 135 billion Euros in 2004 (Andlin-Sobocki *et al.*, 2005).

Currently, to detect the presence of a neurological and neuromuscular disease noninvasively at an early stage is extremely difficult. ALS, also called Lou Gehrig's disease, is a deadly neurodegenerative disease that affects almost selectively motor neurons (Galan *et al.*, 2007). ALS is difficult to diagnose early because the symptoms are similar to those of other, often treatable, neuromuscular disorders where neurodegeneration does not occur. The diagnosis of ALS is usually based on a complete neurological examination and various clinical tests. These tests include muscle related tests and behavior tests. The tests focus on the denervation and reinnervation changes in muscles and the loss of motor neurons in the ALS patients (Fischer *et al.*, 2004).

Large number of experiments focus on the testing of animal models of human's neurological and neuromuscular diseases. Jackson *et al.* (2002) developed superoxide dismutase (SOD) rodent animal models of ALS. Niu *et al.* (2007) employed step-down test to examine the behavioral reaction of the rats with ALS and other diseases like Parkinsonism, which cause extensive damage to the nervous system. The latency of SOD rats was significantly lower than that of controls and the number of performance errors in 5 minutes of exposure was significantly higher than that of the control rats. Since the initial symptoms of ALS are unremarkable, the disease is often undetected in its early stages; however, as more motor neurons fail, the muscles controlled by them stop functioning normally. Eventually, the muscles weaken, become paralyzed, and in most cases, a respiratory failure is the cause of death.

At the present time, there is no effective treatment for ALS. This is due in part to the motor neurons' degeneration and the contributions of other cells, known as glia, towards their demise. Although some drug candidates have been developed, current treatments help alleviate the symptoms but do not stop the progression of the disease (Nicaise *et al.*, 2008). Furthermore, the search for new therapeutic procedures has been hindered by the lack of early and reliable diagnosis. Early detection of ALS is essential for both identifying appropriate candidate animals for inclusion in the treatment group and monitoring the progress and efficacy of the treatment. Thus, early detection and the ability to assess the progression of the disease are critical for the development of new and effective therapeutic treatments for ALS (Babu *et al.*, 2008).

Scientists have tried to develop some ways to detect early symptoms of neurological and neuromuscular locomotion dysfunctions in animal models. Matsumoto *et al.* (2006) published five approaches to detect ALS disease in a rat: body weight, inclined plane, cage activity, SCANET, and righting reflex. They found that the disease progression can be classified into four stages: initiation of motor neuron loss, initiation of body weight loss, onset of muscle weakness, and end-stage disease. Other behavior tests were introduced by Garbuzova-Davis *et al.* (2001) and Offen *et al.* (2009). These behavior tests include:

(i) Extension reflex: Extension of the hindlimbs is observed while a mouse is suspended from its tail. A score (0–2) is given, indicating the number of hindlimbs that are normally extended.

(ii) Rotorod: The number of times that a mouse falls from a rotating axle (3.2 *cm* in diameter at 16 *rpm*) during a 3-*min* period.

(iii) Beam balance: The number of times a mouse crosses a beam (45 *cm* long and 12 *mm* in diameter) during a 3-*min* period.

(iv) Footprint: The mouse leaves a series of footprints on a paper track (50×10 *cm*). Run time, number of steps, distance between fore and hind limbs on left and right sides are measured.

Suzuki *et al.* (2007) found that the onset of ALS was consistently earlier in male than in female superoxide dismutase 1-glycine 93 changed to alanine (SOD1-G93A) rats. They also discovered that SOD1-G93A male rats lost weight more rapidly following the disease onset than SOD1-G93A females; and that motor dysfunction started earlier in males than in females but progressed similarly by testing locomotor

function using the Basso-Beattie-Bresnahan (BBB) rating scale and a beam walking test. Niebroj *et al.* (2007) presented the results of biochemical and electron microscopic (EM) examinations of the spinal cord myelin from SOD1-G93A rats in the early and late symptom-free period of the disease (60 and 93 days of life) and after four-leg paralysis has occurred (120 days of life); biochemical examinations indicated a decrease of lipids, phospholipids, cholesterol and cerebrosides. Thonhoff *et al.* (2007) identified early disease progression in ALS rat models by measuring the peak bodyweight in relation to weight fluctuations.

Muscular injury is not a neurological disease, thus, scientists are interested in studying the recovery mechanisms of muscle injuries (Lovering *et al.*, 2007). Some muscle injuries are caused by a single lengthening contraction (Lovering *et al.*, 2005). Mechanical stabilization is largely imparted by the muscles associated with a joint and can be impaired by muscle strains that are due to sport-related injuries (Garrett, 1996; Best, 1997), labor, or motor vehicle accidents (Kettler *et al.*, 2002; Brault *et al.*, 2000). The animal model of neuromuscular injury is induced by repeated large strain lengthening contractions of the dorsiflexors muscles as shown in Figure 1.1.

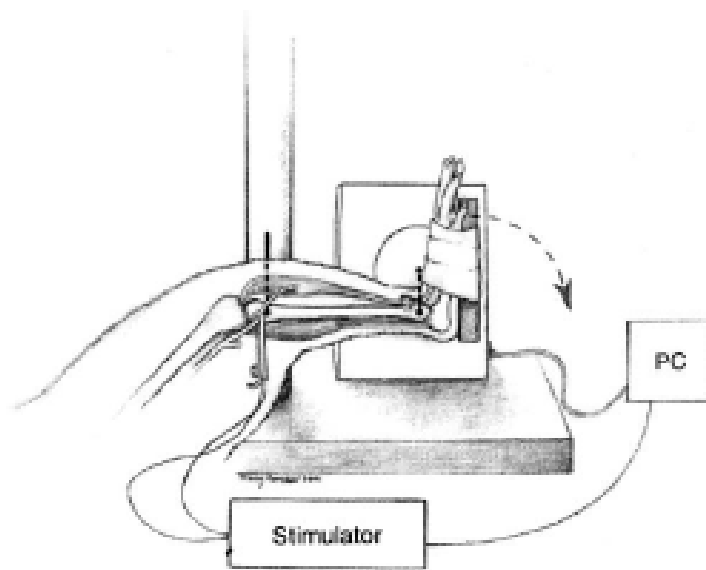


**Figure 1.1** Muscle Injury Model: the tibia of the hindlimb was stabilized and the foot secured to a plate driven by a stepper motor. The peroneal nerve was used to stimulate the TA anterior (a dorsiflexor) at a selected time while the plate forced the foot into plantar flexion at a selected velocity (Lovering *et al.*, 2005).

Similarly to ALS, Parkinson's disease (PD) is difficult to diagnose in its early stages. PD is one of the most common chronic neurodegenerative diseases. The main symptoms of PD are bradykinesia, rigidity, rest tremor and postural instability (Twelves *et al.*, 2003). Researchers have contributed a number of findings to help investigate PD. Two rodent models, which are methyl-phenyl-tetrahydro-pyridine (MPTP) treated mice and 6-Hydroxydopamine (6-OHDA), are widely used for research purposes of this disease (Schober 2004). Muir and Wishaw (1999) have studied the behavioral differences between the 6-OHDA rats and control rats by using a miniature force platform as shown in Figure 1.2. The center of the weight of 6-OHDA rats could not follow a sine wave whereas the center of weight of control rats followed it at the walk, as shown in Figure 1.3 (a). The sum of the vertical ground reaction forces (GRFs) from the diagonal legs has only one peak for the control and



more for the 6-OHDA (see Figure 1.3 (b)). Yet, the methods listed above cannot detect PD early.

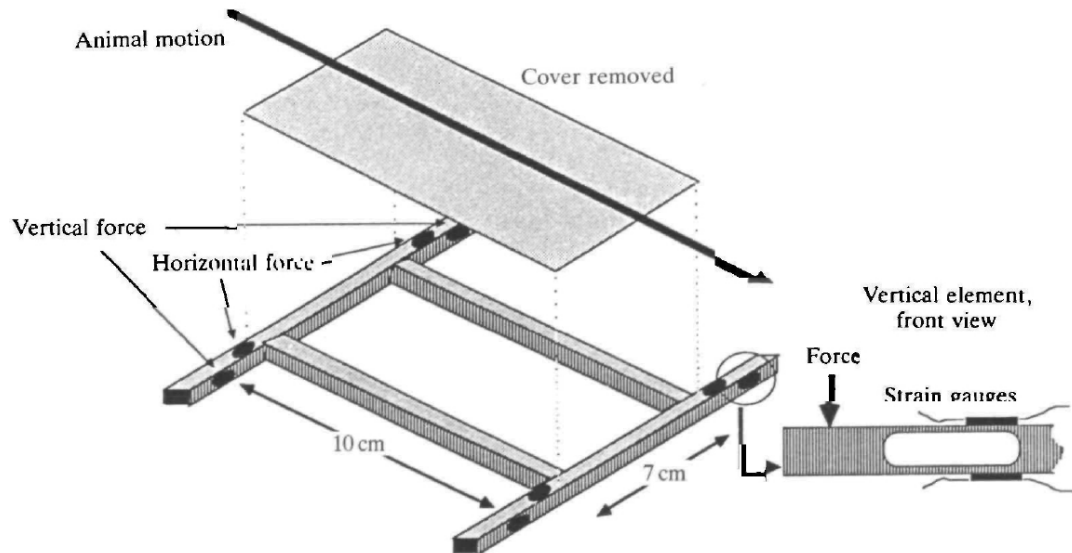


**Figure 1.2** Miniature force platform. Semiconductor strain gauges mounted on spring blades are sensitive to vertical and horizontal deformation of the beams caused by forces exerted when the animal moves over the wooden cover (Full and Tu, 1990).

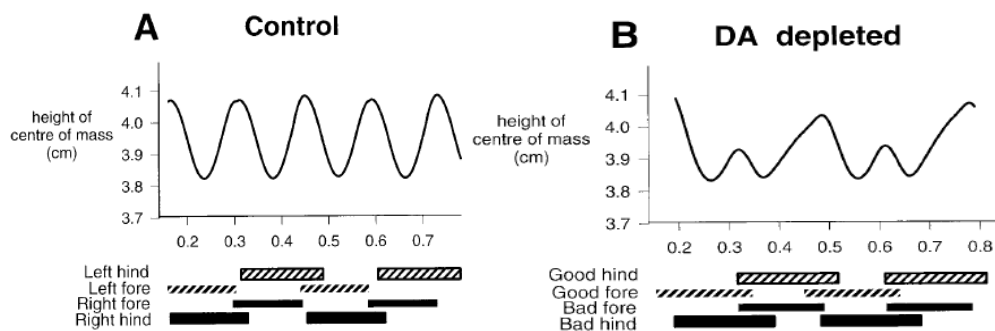


**Figure 1.3 (a)** By measuring the ground reaction forces in vertical direction, it was found that the mass center of a control rat followed a sine wave when the rat was walking while Parkinson's rats didn't (Muir and Whishaw, 1999).

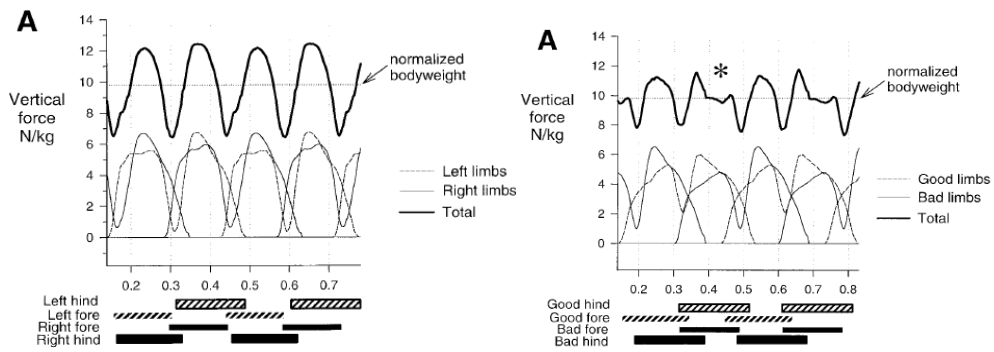


**Figure 1.3 (b)** By measuring the ground reaction forces in vertical direction, it was found that the sum of the forces from diagonal legs during about the same period of time has only one peak for control rats while the rats with Parkinson's disease have more than one peaks (Muir and Whishaw, 1999).

Despite all the research methods above, neither muscles related tests nor behavior tests are able to detect the disorders due to PD early and accurately enough. Gait analysis systems have been widely used to detect neurological and neuromuscular diseases due to its simple implementation, low cost, reduced complication and non-invasive procedure (Neumann *et al.*, 2009; Hamers *et al.*, 2001; Koopmans *et al.*, 2006). A digital imaging system called DigiGait™, shown in Figure 1.4, was developed by Mouse specifics, Inc. (Hampton *et al.*, 2004; Wooley *et al.*, 2005; Li *et al.*, 2005). A mouse or a rat is put on the transparent treadmill enclosed in a compartment. The treadmill belt maximizes the efficiency of the camera and image processing software to identify paw contact with the treadmill surface at various walking and running speeds. Eleven gait parameters, listed in Table 1.1, can be generated in time and space domains.



**Figure 1.4** DigiGait™ made by Mouse Specifics Inc. The system has a treadmill on the bottom of the transparent compartment. The speed of the treadmill and the size of the compartment are adjustable. A video camera records bottom images of the rat that walks through the system. All the locomotion parameters are generated from the analysis of the images.

Table 1.1 Description of gait parameters that were used to evaluate change in gait following intraarticular injection of carrageenan by DigiGait™. (Berryman *et al.*, 2009)

<b>Gait Indices</b>	<b>Description</b>
1. Swing Time (sec)	The forward portion of the stride during which the paw is not in contact with the belt
2. Stance/Swing (ratio)	The ratio of Stance time to Swing time
3. Braking Time (sec)	The time between initial paw contact with the belt to the maximal paw contact
4. Stance Time (sec)	The portion of the stride in which the paw remains in contact with the belt
5. % Stance/Stride	The percent of time that the Stance Time contributes to one complete Stride cycle
6. Stride Length (cm)	The distance between initial contacts of the same paw in one complete stride
7. Stride Time (sec)	The amount of time to complete one complete stride for one limb
8. % Swing/Stride	The percent of time that the Swing Time contributes to one complete Stride cycle
9. % Propulsion/Stride	The percent of time that the Propulsion Time contributes to one complete Stride cycle
10. Paw Area (cm <sup>2</sup> )	The maximal paw area in contact with the treadmill during the stance phase of the step cycle
11. Stance Width (cm)	The distance between the two front feet or the two hind feet as measured from the middle of the paw area

Similarly, Noldus information technology has a gait analysis system called CatWalk™, shown in Figure 1.5 (Noldus IT, 2006). CatWalk™ is also a video-based system used to assess locomotion deficits and pain-induced gait adaptations in voluntarily walking mice or rats. Gait parameters listed in Table 1.2 can be generated by this system.



**Figure 1.5** CatWalk™ invented by Noldus Information Technology. The floor of the system is transparent and lightened by arrays of LED. Only at the points where a paw touches the glass, light exits the floor and scatters at the paw, illuminating the points of contact only (Noldus IT, 2006).

Table 1.2 Description of gait parameters that were used to evaluate change in gait by CatWalk™. (Neumann *et al.*, 2009; Deumens *et al.*, 2007)

<b>CatWalk Parameters</b>	<b>Explanation</b>
1.Base-of-support (BOS)	Distance between two hindpaws, as measured perpendicular to the waling direction
2.Stride length (cm)	Distance between the placement of a hindpaw and the subsequent placement of the same paw
3.Box length	Length of the box which is artificially placed around the paw prints by the CatWalk™ software program
4.Box width	Width of the box which is artificially placed around the paw prints by the CatWalk™ software program
5.Maximum area	Total surface area of the glass floor contacted by the hindpaw at the moment of maximum paw-floor contact during the stance phase of the hindpaw
6.Print area	Total surface area of the glass floor contacted by the hindpaw during the complete stance duration
7.Mean intensity	Mean intensity of the pixels forming the maximum area
8.Stance duration	Time of contact of the hindpaw with the glass floor
9.Swing duration	Time that the hindpaw is not in contact with the glass floor
10.Regularity index (RI)	An index for the degree of interlimb coordination during gait, as measured by the number of normal step sequence patterns (NSSP). Multiplied by four (number of paws), divided by the number of paw placements, and multiplied by 100%; $RI = (NSSP \times 4) / \text{number of paw placements} \times 100\%$ . With respect to RI six NSSP have been previously described (Cheng <i>et al.</i> , 1997) and involve cruciate, alternate, and rotary step patterns
11.Phase lags	Parameters that appreciate the timing relationships between paw placements. The time of initial contact of one paw (the target) is related (expressed as a percentage) to the stride length of another paw (the anchor). Phase lags can be calculated between the paws of the same girdle (forepaws or hindpaws), between paws on the same side (ipsilateral left or ipsilateral right), and between diagonal paws (opposite forepaw/hindpaw)

According to Table 1.1 and Table 1.2, it is obvious that DigiGait™ and CatWalk™ can only measure gait parameters that are in time and space domains. Due to this limitation, some gait abnormalities which affect the ground reaction forces

may not be able to be detected by either DigiGait™ or CatWalk™ (Guillot *et al.*, 2008).

In addition, both DigiGait™ and CatWalk™ only provide a series of gait parameters to the users (Bozkurt *et al.*, 2008). It depends on the user how the parameters are to be handled. Nevertheless, most users wish to know if a tested animal has a certain disease and do not desire to examine multiple numbers of gait parameters. Neither DigiGait™ nor CatWalk™ can provide such detection. Guillot *et al.* (2008) reported that a computerized gait analysis system or DigiGait™ was unable to consistently identify motor problems in MPTP-treated mice, despite a 90% deficit of striatal dopamine content. In addition, the same gait analysis system could not distinguish SOD1-G93A, a mouse model of ALS, from controls up to 84 days of age.

## **1.2 Objectives and Specific Aims**

Many experimental studies proved that gait analysis is an effective method for preliminarily analyzing gait impairments (Lin *et al.*, 2008; Gabriel *et al.*, 2007). However, there are still challenges neuroscientists and engineers are faced with when this approach is implemented. The model to calculate the probability of a tested animal has a neurological disorder is not available. Thereby, it is difficult to provide a yes/no result. An effective way to find the “proper” locomotion parameters that constitute biomarkers of the disease one investigates has not yet been found. The research in this dissertation focuses on providing better methodology for performing gait analysis.

The main objective of this work is to detect neurological and neuromuscular diseases in an early stage by using an in house Gait Analysis System (GAS) in

laboratory rats. There are three specific aims:

(1) Improve the hardware and software (Moubarak, 2007) of an in house gait analysis system developed for equines by Keny (2005).

(2) Develop an effective methodology to detect gait impairments.

(3) Test the developed methodology by running a series of laboratory experiments.

### **1.3 Dissertation Overview**

This dissertation contains six chapters written in a chronological order following the performance of the work. Chapter 2 describes the developed methodology to detect gait abnormalities, including hardware, software (Tasch *et al.*, 2008) and statistical methods. Chapter 3 describes the experiment to distinguish SOD1-G93A rats from the control (Tang *et al.*, 2009a). Chapter 4 is based on the hypothesis that the severity of an injury can be assessed by using the gait analysis system (Tang *et al.*, 2009b). Chapter 5 describes an experiment in which (Tang *et al.*, 2010) rats injected with 6-OHDA to model Parkinson's disease. At last, Chapter 6 summarizes the results presented in the preceding chapters along with future work and proposed further research.

## Chapter 2: Methodology

An in house Gait Analysis System (GAS) was set up to measure Ground Reaction Forces (GRFs) and spatial limb positions associated with individual limbs through the synchronization of load-cell records and video images. Three logistic regression models are derived to predict ALS disease, to test the recovery of injury, and to detect the outcome of Parkinson's disease using Locomotion Parameters (*LPs*) (Tang *et al.*, 2009a, 2009b, 2010). By calculating the probability of a tested animal being a diseased one and setting the cutoff value, a clear picture can be attained whether the tested animal has a disease or not.

### 2.1 Gait Analysis System

GAS was originally designed by Keny (2005) and the corresponding software was developed by Moubarak (2007). GAS can measure GRFs of vertical, longitudinal, and transverse directions measured by fourteen load-cells: eight load-cells measure vertical GRF components (*Z*), two load-cells measure longitudinal GRF components (*Y*) and four measure transverse GRF components (*X*). The software that records the data from the fourteen load-cells and the software for analyzing the forces have been improved by the author. The hardware and the developed software records and analyzes GRF and spatial (longitudinal and transverse) limb positions data of a walking laboratory rat.



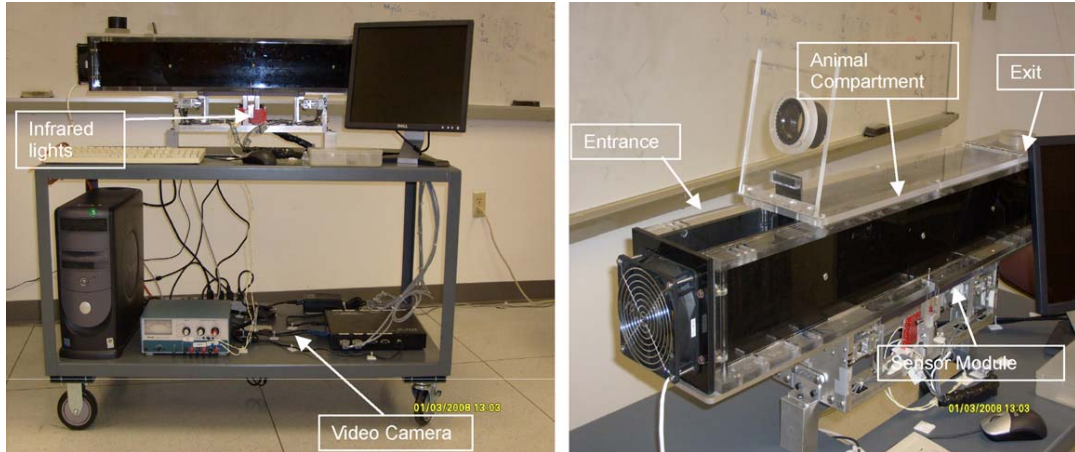


**Figure 2.1** A gait analysis system for rodents. The system measures LPs in 4 domains: force, space, time, and frequency. The measured forces are in vertical, longitudinal, and transverse directions. A video camera records bottom images of the rat that walks through the system, and through synchronization of the video images and load cell signals, one can recognize the ground reaction forces of each individual limb.

The GAS went through several enhancements. First, it was mounted on a steel cart to improve its mobility (see Figure 2.1). Second, two highly sensitive load-cells (Transducer Techniques, 150 grams #206757) were mounted to measure the longitudinal GRF components. Third, a digital video camera (Sony, DMK 31BF03) was installed on the bottom shelf to record the bottom view of the walking rats. To control the lighting, two arrays of infrared LEDs were set up on the edge of the sensor module plates (Tasch *et al.* 2008). The two plates of the floor were shortened and the entrance and the exit plates were extended. In addition, the material of the floor was changed from Aluminum to transparent plastic (Plexiglas). The locations of the two load-cells that measure longitudinal GRF components were changed from the center to the two sides. These enhancements resulted in a GAS that records video images as well as vertical, longitudinal, and transverse GRFs and spatial (longitudinal and

transverse) limb positions of walking rats. The load-cell data is collected at a rate of 200 Hz and the video is recorded at 30 frames per second.

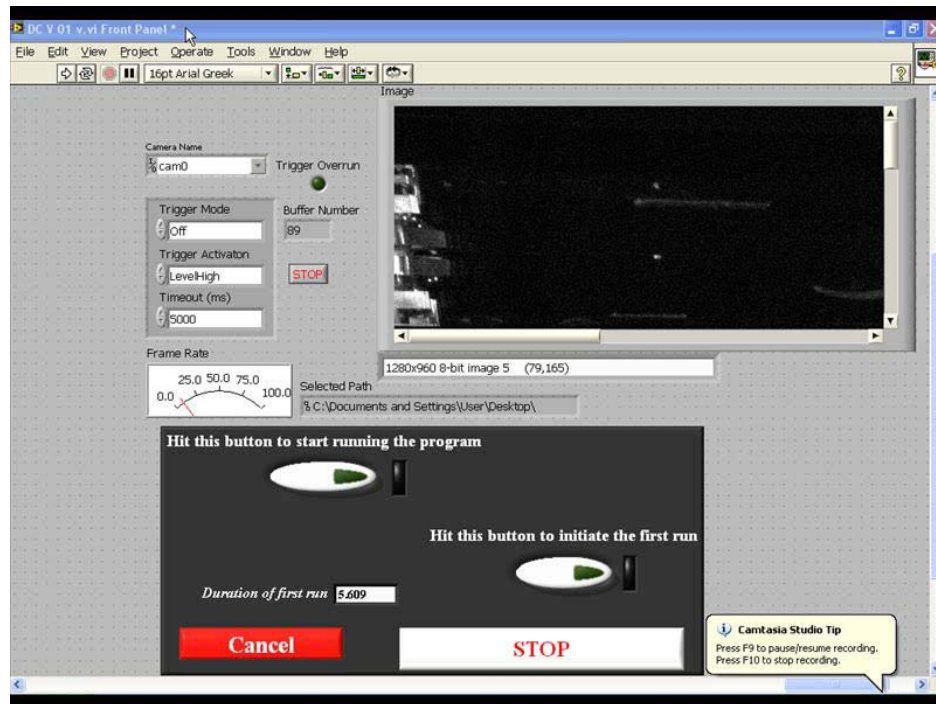


**Figure 2.2** The new version of data collection software for gait analysis system programming by LabVIEW<sup>®</sup>. Forces data and the video data start to be collected at the same time when the data collection software is run. As soon as the software is stopped, there will be two files created in a specific folder automatically, which store force data and video images.

The video collection unit was added to the data collection software by using a LabVIEW<sup>®</sup> 8.5 program (see Figure 2.2). The GRF and the video data start to be collected at the same time when the data collection software is clicked to run. As soon as the software is stopped, two files are automatically created in a specific folder: one is a “.txt” file which is used to store GRF data and the other one is an “.avi” file that stores video images. A screen, a frequency meter, and some other function blocks were added to the front panel of the data collection software. This control panel aids the user in observing how the rat walks through the system.

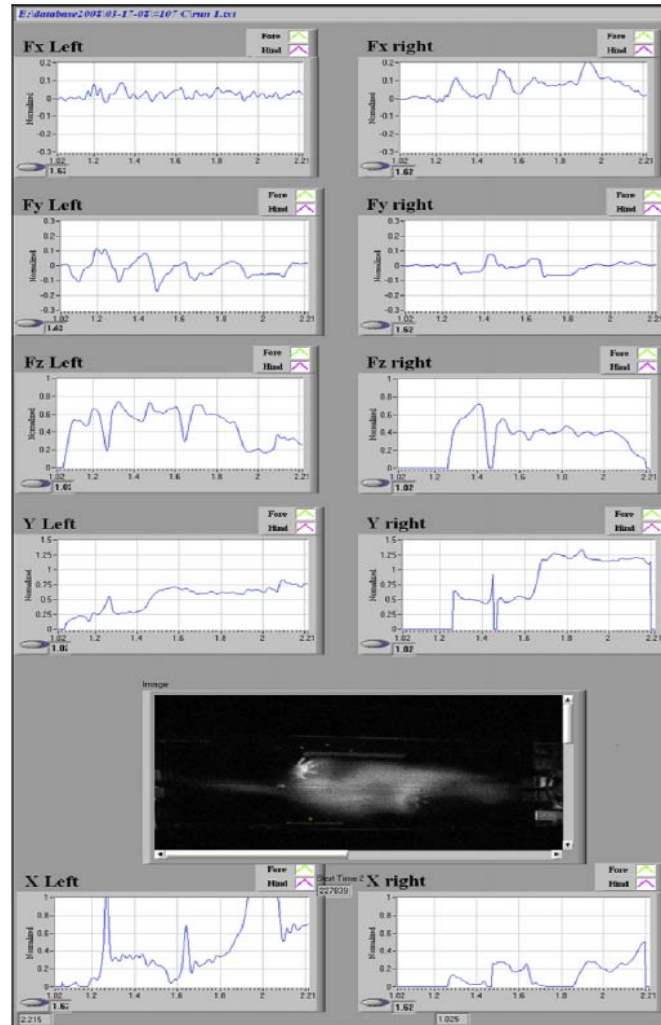


**Figure 2.3** A typical output generated by the GAS from a typical test run. The signatures of the left and right limbs are depicted on the left and right sides. The transverse ( $F_x$ ), longitudinal ( $F_y$ ), and vertical ( $F_z$ ) are normalized with respect to the rat's body weight and plotted as a function of time ( $s$ ). The longitudinal ( $Y$ ) and transverse ( $X$ ) limb positions are normalized with respect to the length and width of the floor plates, respectively. A video image of the bottom of the rat is also recorded.

The data analysis software has also been modified. A display that can play images recorded by the data collection software was added to the front panel of the data analysis software (see Figure 2.3), and a corresponding program was added to the block diagram. The images and GRF data were synchronized to achieve a better understanding of how a rat walks through the GAS. Four cursors (see Figure 2.4)

were also synchronized in  $Fz$  and  $Y$  positions both left and right sides. The video can be played forward and backward by moving the cursors. The output signals of the fore and hind limbs are designated by dashed and solid lines, for both left and right floor plates. The processed system outputs (see Figure 2.5) allow the user to associate the system outputs with individual limbs, and to calculate numerous  $LPs$  that characterize the locomotion of a rat through each limb for every test run.

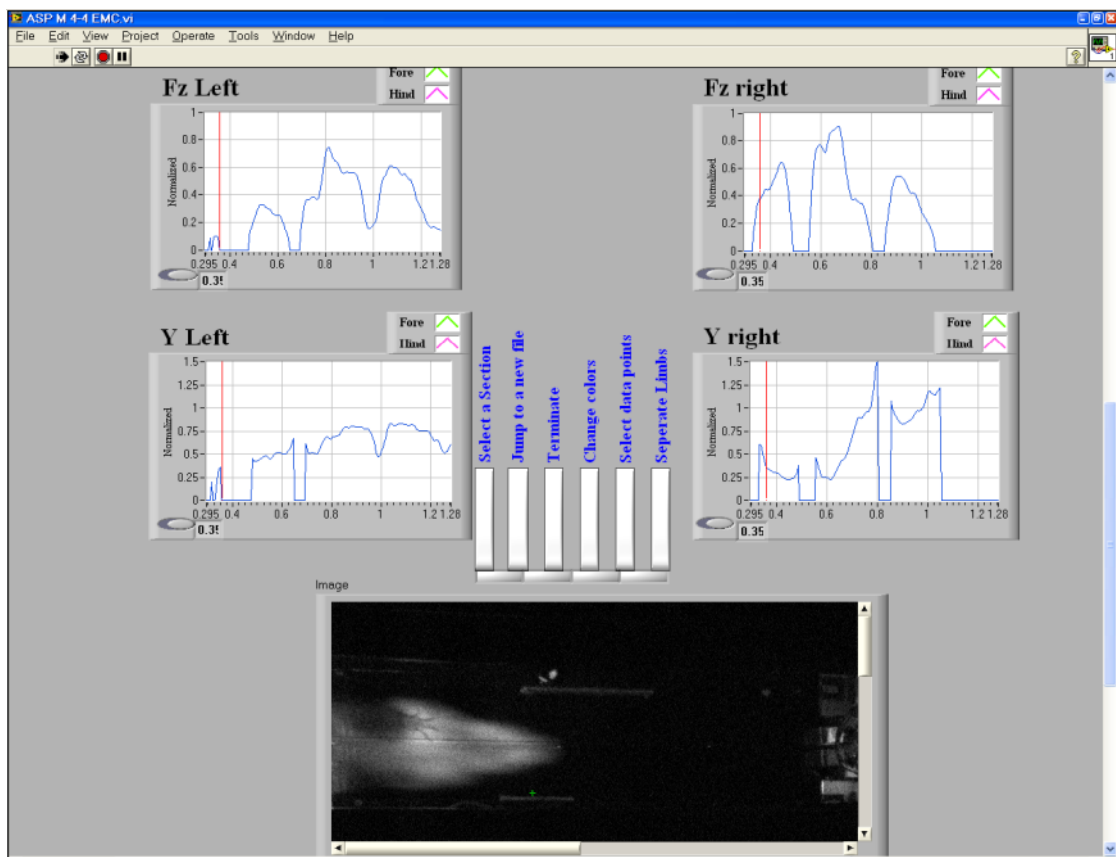


**Figure 2.4** To associate a load-cell signature with a limb, the computer mouse is placed on a selected signature (vertical marker); and the most recent video image is displayed. The load-cell signature on the right from 0.36 to 5.0 s is associated with the right fore limb.

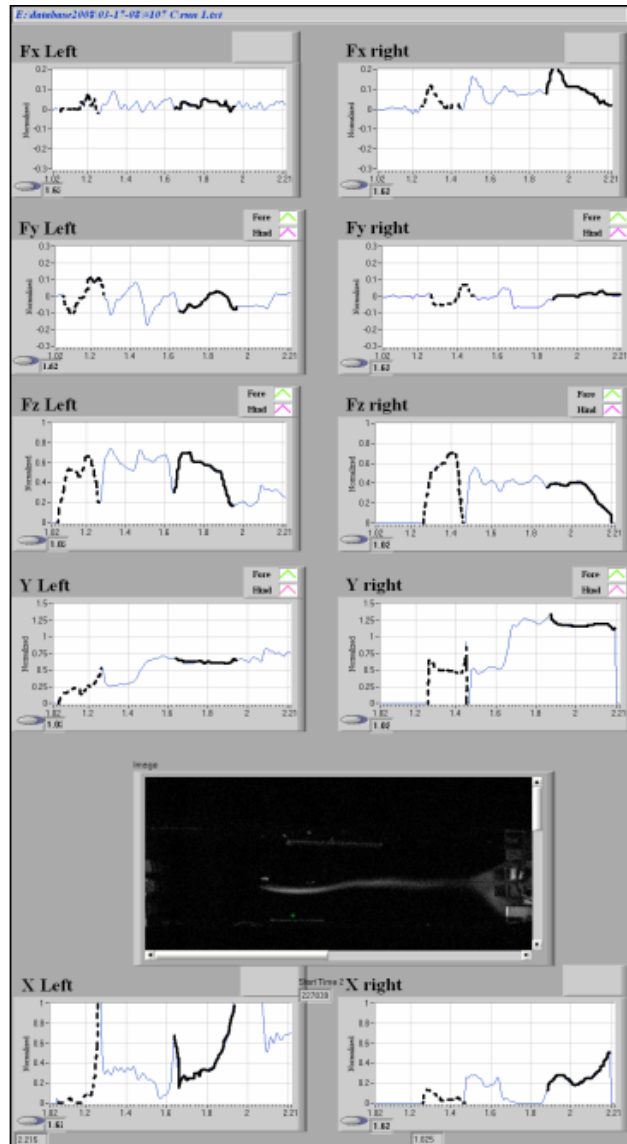


**Figure 2.5** The load signatures generated by a single limb are identified and following the procedure shown in Figure 2.4, the fore and hind limbs are marked with dashed and solid heavy lines, respectively.

## 2.2 Locomotion Parameters (LPs)

From the signals of the 14 load cells, the values of 20 LPs per limb were evaluated for the Left Fore (LF), Right Fore (RF), Left Hind (LH), and Right Hind (RH) limbs. The 20 LPs, listed in Table 2.1, are non-dimensional except to *Stance Time*,  $F_{zw}$  and  $F_y$  which have dimensions of  $s$ ,  $l/s$ , and  $l/s$ , respectively.

Table 2.1 Definitions of the 20 LPs evaluated in this dissertation.

No.	Variable	Units	Definition
1	$F_{z_{max}}$	Non-dimensional	Maximum value of the vertical GRF component of a selected limb
2	Stance Time	sec	Time duration that a selected limb is in contact with the floor
3	$T_{F_{z_{max}}}$	Non-dimensional	Time of $F_{z_{max}}$ normalized by the Stance Time of a selected limb
4	$F_{z_{mean}}$	Non-dimensional	The mean value of the vertical GRF component of a selected limb $\left[ \frac{\int_{S.Time} F_z \cdot dt}{StanceTime} \right]$
5	$F_{zw}$	1/sec	The Fourier transform of $F_z$ summed over the first 50 Hz for a selected limb $\limb \left[ \int_{50} F_z \cdot d\omega \right]$
6	Stride	Non-dimensional	Stride length of a selected limb calculated as the difference between two consecutive contact positions; the contact positions are normalized by the floor length, which is 13.25 inch
7	$F_{y_{max}}$	Non-dimensional	Maximum value of the longitudinal GRF component of a selected paw
8	$T_{F_{y_{max}}}$	Non-dimensional	Time of $F_{y_{max}}$ divided by Stance Time
9	$F_{y_{min}}$	Non-dimensional	Minimum value of the longitudinal GRF component of a selected paw
10	$T_{F_{y_{min}}}$	Non-dimensional	Time of $F_{y_{min}}$ divided by Stance Time
11	$F_{y_{mean}}$	Non-dimensional	The average value of the longitudinal GRF component of a selected paw $\left[ \frac{\int_{S.Time} F_y \cdot dt}{StanceTime} \right]$

12	Fyw	1/sec	The Fourier transform of Fy summed over the first 50 Hz for a selected paw $\left[ \int_{50} Fy \cdot d\omega \right]$
13	Fx <sub>max</sub>	Non-dimensional	Maximum value of the transverse GRF component of a selected paw
14	Fx <sub>min</sub>	Non-dimensional	Minimum value of the transverse GRF component of a selected paw
15	Fx <sub>mean</sub>	Non-dimensional	The average value of the transverse GRF component of a selected paw $\left[ \frac{\int_{S.Time} Fx \cdot dt}{S \tan ceTime} \right]$
16	FyP	Non-dimensional	The mean value of the propelling (positive) longitudinal force of a selected limb
17	FyB	Non-dimensional	The mean value of the braking (negative) longitudinal force of a selected limb
18	NP	Non-dimensional	The number of samples in which the longitudinal force is propelling (positive in value); the sampling rate is 200 Hz
19	NB	Non-dimensional	The number of samples in which the longitudinal force is braking (negative in value); the sampling rate is 200 Hz
20	NPB	Non-dimensional	The number of times in which the longitudinal force switches sign from braking to propelling and vice versa

### 2.3 Logistic Regression Model

In an earlier work Rajkondawar *et al.* (2002) addressed modeling of bovine lameness, using a logistic regression to evaluate lameness predictions of dairy cattle. Logistic regression model (Hosmer and Lemeshaw, 2000) has been used to predict the probability that an examined rat belongs to the diseased mutant group in terms of the  $LP$ . The model is expressed mathematically as:

$$P(\text{a rat} \in \text{diseased group}) = \frac{\exp(\beta_0 + \sum \beta_i \cdot LP_i)}{1 + \exp(\beta_0 + \sum \beta_i \cdot LP_i)} \quad , \quad (2.1)$$

where  $\beta_0$  is the intercept and  $\beta_i$  is the  $i$ -th coefficient of the logistic regression model and is estimated by appropriate statistical methods. Liu *et al.* (2009) demonstrated that the accuracy of the predictions of such models is significantly improved when the  $LP$ s are transformed via spline transformations. An implementation of these transformations is available in SAS (PROC TRANSREG) (SAS Institute Inc., 2004). The probability that a rat belongs to the diseased mutant group is hence evaluated as:

$$P(\text{a rat} \in \text{diseased group}) = \frac{\exp(\beta_0 + \sum \beta_i \cdot TLP_i)}{1 + \exp(\beta_0 + \sum \beta_i \cdot TLP_i)} \quad , \quad (2.2)$$

where  $TLP_i$  is the transformed value of  $LP_i$ .

### 2.4 Animal Protocols

All protocols described in this study were approved by IACUC at the University of Maryland, Baltimore County and the University of Maryland, School of Medicine.



At the end of our experiments, animals were euthanized by sodium pentobarbital injection (150 mg/kg IP).

## Chapter 3: Measuring Early Pre-symptomatic Changes in Locomotion of Rodent Models of SOD1-G93A- a Rodent Model of Amyotrophic Lateral Sclerosis

### 3.1 Introduction to the Rodent ALS Models

This chapter demonstrates that to differentiate SOD1-G93A mutant rat, a model of Amyotrophic Lateral Sclerosis (ALS), from a Sprague Dawley (SD) control rat at a pre-symptomatic stage, one has only to use 7 key parameters. The 7 parameters are biomarkers of ALS and their transformed values are used as explanatory variables of a logistic regression model. The model predicts the probability that the examined rat belongs to the SOD1-G93A group. This model differentiates faultlessly between the SOD1 and control groups from the very first time rats, 51 days of age, walked through the system. The system provides a new paradigm for ALS diagnosis and it can have a significant impact on the development of new therapeutic procedures for this ailment. It is further possible to address the development of therapeutic procedures for other neurological diseases that affect gait.

ALS is a serious neurodegenerative disease that affects almost selectively motor neurons (Galan *et al.*, 2007). ALS is also called Lou Gehrig's disease and is very difficult to diagnose in the early stages because the symptoms are similar to those of other, often treatable, neuromuscular disorders where neurodegeneration does not occur. The diagnosis of ALS is usually based on a complete neurological examination and various clinical tests. Since the initial symptoms of ALS are unremarkable, the disease is often undetected in its early stages. However, as more motor neurons fail,

the muscles controlled by them stop functioning normally. Eventually, the muscles weaken and become paralyzed and, in most cases, a respiratory failure is the cause of death.

At the present time, there is no effective treatment for ALS. This is due in part to the motor neurons' degeneration and the contributions of other cells, known as glia, towards their demise. Current treatments help control the symptoms but they do not stop the progression of the disease or cure it. Furthermore, the search for new therapeutic procedures has been hindered by the lack of early and reliable diagnosis. Early detection of ALS is essential for both identifying appropriate candidate animals for inclusion in the treatment group and monitoring the progress and efficacy of the treatment. Thus, early detection and the ability to assess the progression of the disease are critical for the development of new and effective therapeutic treatments for ALS.

Laboratory animal models have been used to study the progression of ALS in rats and mice. SOD1-G93A rats (Howland *et al.*, 2002) have been accepted as animal model for ALS due to their similarities to human ALS symptoms, including muscle weakness, weight loss, chewing reflex, paralysis, and breathing difficulties.

Researchers have investigated motor symptoms that detect ALS early. Kafkafi *et al.* (2008) reported that a Pattern Array for data mining of movement distinguishes control SD rats from SOD1-G03A mutant rats. The former exhibit heavy breaking when moving along an arena wall and turning away from it, whereas the SOD1-G93A mutants fail to exhibit this behavioral pattern. According to Kafkafi *et al.* (2008), these symptoms may enable researchers to test therapies that address intervention rather than remediation.

This chapter describes a quantitative method to detect the presence or absence of locomotion dysfunction in a rodent model of ALS. The diagnosis is based on a number of *LPs* generated at each stride of every limb as the animal walks freely through a narrow passage to get food placed at the system exit. Using several repeated walks of animals with known disease conditions, we build predictive models for ALS in terms of *LPs* that have been transformed through spline transformations (Liu *et al.*, 2008). The transformed *LPs* are used as explanatory variables of a logistic regression model for the probability that the examined rat belongs to the SOD1-G93A mutant group.

The GAS (see Figure 2.1), described in the Chapter 2, can measure numerous locomotion parameters for every test run. In this chapter 110 locomotion parameters per animal per run are evaluated for their ability to identify the presence of the disease. For each *LP*, we explore a nonlinear transformation based on spline functions, which best predict the presence of ALS. It is demonstrated that in order to classify SOD1-G93A rats correctly one has to measure only 7 very particular *LPs* per limb. It turns out that the system is capable of distinguishing between the SOD1 mutants and control SD animals correctly from the very first time the animal crosses the system.

## **3.2 Materials and Methods**

### **3.2.1 Obtaining Gait Measurements for the ALS Experiment**

Four SOD1-G93A mutant and four Sprague-Dawley (SD) control rats from Taconic Laboratory (Germantown, NY) participated in the study. The rats were all males and 4 weeks old upon their arrival on Jan 7, 2008. Each rat was housed in a separate cage with inversed darkness/lighting cycle and food and water *ad libitum*.

After weighing the animal it was placed at the system entrance, the gate was opened, and the rat crossed the system moving toward its individual cylindrical toy and a treat of condensed milk, both of which were placed at the system exit. This procedure was repeated up to 3 times for each rat on a single day. After a period of 10 days of training and adaptation to the system, each animal was tested twice per week and data was recorded from January 30, when the rats were 51 days old, through March 24, 2008 or until the rats were 105 days of age. The database contained 163 test runs, where 96 records were from SOD1 mutants and 67 from control SD rats.

### 3.2.2 Logistic Regression

In the Chapter 2, the logistic regression model was introduced. In the current chapter, logistic regression models are used to predict the probability that an examined rat belongs to the SOD1-G93A mutant group in terms of the  $LPs$ . This is expressed mathematically as:

$$P(\text{a rat} \in \text{SOD1 group}) = \frac{\exp(\beta_0 + \sum \beta_i \cdot LP_i)}{1 + \exp(\beta_0 + \sum \beta_i \cdot LP_i)}, \quad (3.1)$$

where the  $\beta_i$  is the  $i$ -th coefficient of the logistic regression model and is estimated by appropriate statistical methods.

### 3.2.3 Cross Validation

Leave-One-Out (Efron and Tibshirani, 1993; Hjorth, 1994) method of cross validation was used to evaluate the performance of the derived ALS models. A single test run from the original sample is taken as the validation data, and the remaining

test runs are taken as the training data. This procedure is repeated 163 times until every test run in the database is used once as the validation data.

### 3.3 Results of the ALS Experiment

A typical output of a single test run is depicted in Figure 2.3. These outputs are recorded from an array of fourteen load cells that support the left and right floor plates of the system sensor module, as described in Tasch *et al.* (2008). Vertical ( $F_z$ ), longitudinal ( $F_y$ ), and transverse ( $F_x$ ) GRF components, as well as longitudinal ( $Y$ ) and transverse ( $X$ ) limb positions, are plotted versus time ( $s$ ) for both left and right floor plates. In addition, bottom images of the walking rat are recorded by a video camera.  $F_z$ ,  $F_y$ , and  $F_x$  are normalized with respect to the animal's body weight, and the longitudinal ( $Y$ ) and transverse ( $X$ ) limb positions are normalized with respect to the length and width, respectively of the sensor module floors. Thus  $Y = 0$  denotes the entrance, and  $Y = 1$  denotes the exit, where  $X = 0$  denotes the center line and  $X = 1$  the far edge (see Figure 2.3).

At any time the left and right floors can be in contact with one, two, or no limbs. When a single limb is in contact with the floor plate, we synchronize the load cell outputs that are recorded at 200 *Hz*, with the most recent video image recorded at 30 *fps*. This enables us to verify the association between an individual limb and a recorded force signature. Figure 2.4 demonstrates that the output signatures of the right floor plate during the time period of 0.36 to 0.5 *s* are generated when the right fore limb is in contact with the right floor plate. Similarly, one can associate the other limbs with the load cell signals they generate. Thus each fore and hind limb is designated with dashed and solid lines, respectively (Figure 2.5). This enables one to

calculate numerous *LPs* that characterize the locomotion of a rat through each limb for every test run.

Table 2.1 lists the 20 *LPs* that were evaluated for every limb in this chapter. The list includes gait parameters that characterize the vertical ( $Fz$ ), longitudinal ( $Fy$ ) and transverse ( $Fx$ ) forces, as well as parameters that are associated with time, stride, and frequency ( $Fz$ , and  $Fy$ ). In addition to the 20 *LPs*, listed in Table 2.1, we derived parameters that capture symmetry between the left and right sides of the animal. This is based on the hypothesis that control rats exhibit left/right *LP* symmetry. Symmetry of any locomotion parameter is defined as:

$$Sym\_LP = \frac{LP_{left} - LP_{right}}{LP_{left} + LP_{right}}. \quad (3.2)$$

Equation (3.2) can be applied to any of the 20 *LPs* listed in Table 3.1. Symmetry can be evaluated for the hind ( $Sym\_LP_H$ ) or the fore ( $Sym\_LP_F$ ) limbs. The symmetry factors, listed in Table 3.1, were evaluated for the fore and hind limbs in this chapter.

The 20 *LPs*, listed in Table 2.1, were evaluated for LF, RF, LH, and RH limbs and the symmetry factors, listed in Table 3.2, were evaluated for the forelimbs and hindlimbs for every test run of the 4 control and 4 SOD1-G93A rats. A typical data for a single test run contained values of 110 parameters, as depicted in Table 3.2.

Table 3.1 Definitions of 15 symmetry factors.

No.	Variable	Units	Definition
1	Sym_Fz <sub>max</sub>	Non-dimensional	<i>The Symmetry factor of Fz<sub>max</sub></i>
2	Sym_Stance Time	Non-dimensional	<i>The Symmetry of Stance Time</i>
3	Sym_T_Fz <sub>max</sub>	Non-dimensional	<i>The Symmetry of T_Fz<sub>max</sub></i>
4	Sym_Fz <sub>mean</sub>	Non-dimensional	<i>The Symmetry of Fz<sub>mean</sub></i>
5	Sym_Fzw	Non-dimensional	<i>The Symmetry of Fzw</i>
6	Sym_Stride	Non-dimensional	<i>The Symmetry of Stride</i>
7	Sym_Fy <sub>max</sub>	Non-dimensional	<i>The Symmetry of Fy<sub>max</sub></i>
8	Sym_T_Fy <sub>max</sub>	Non-dimensional	<i>The symmetry of T_Fy<sub>max</sub></i>
9	Sym_Fy <sub>min</sub>	Non-dimensional	<i>The symmetry of Fy<sub>min</sub></i>
10	Sym_T_Fy <sub>min</sub>	Non-dimensional	<i>The symmetry of T_Fy<sub>min</sub></i>
11	Sym_Fy <sub>mean</sub>	Non-dimensional	<i>The symmetry of Fy<sub>mean</sub></i>
12	Sym_Fyw	Non-dimensional	<i>The symmetry of Fyw</i>
13	Sym_Fx <sub>max</sub>	Non-dimensional	<i>The symmetry of Fx<sub>max</sub></i>
14	Sym_Fx <sub>min</sub>	Non-dimensional	<i>The symmetry of Fx<sub>min</sub></i>
15	Sym_Fx <sub>mean</sub>	Non-dimensional	<i>The symmetry of Fx<sub>mean</sub></i>



Table 3.2 Numerical values of the 20 measured *LPs* for each (LF. RF. LH. RH) limbs and the 15 symmetry factors for fore and hind limbs for a control rat #107.

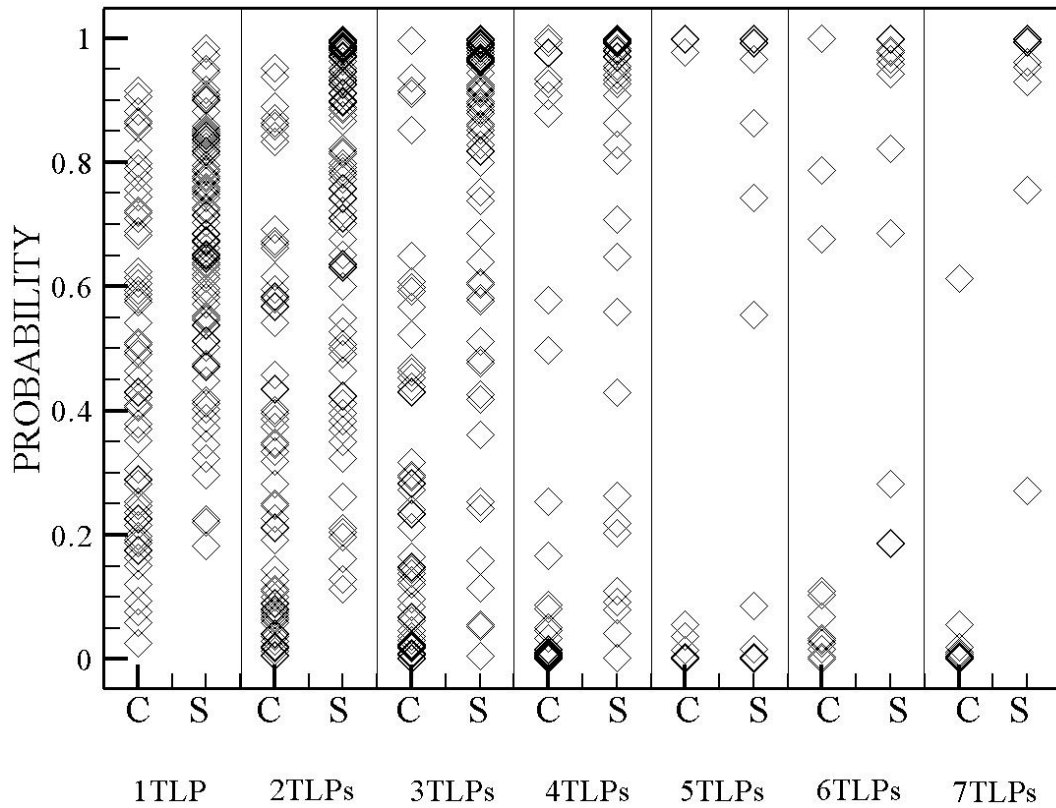
<b>Locomotion Parameter (LP)</b>	<b>LF</b>	<b>RF</b>	<b>LH</b>	<b>RH</b>	<b>Sym_LP<sub>F</sub></b>	<b>Sym_LP<sub>H</sub></b>
Fz <sub>max</sub>	0.7398	0.8116	0.7357	0.7254	-0.046	0.007
Stance time [sec]	0.1550	0.1400	0.2900	0.1750	0.051	0.247
T_Fz <sub>max</sub>	0.3226	0.7500	0.2241	0.2857	-0.398	-0.121
Fz <sub>mean</sub>	0.5288	0.5260	0.4221	0.3918	0.003	0.037
Fz [1/sec]	0.5326	0.5280	0.5194	0.4605	0.004	0.060
Stride	0.3463	0.7202	0.4133	0.6818	-0.351	-0.245
Fy <sub>max</sub>	0.1517	0.3986	0.0178	0.3771	-0.449	-0.910
T_Fy <sub>max</sub>	0.8710	0.1786	0.5172	0.4571	0.660	0.062
Fy <sub>min</sub>	-0.4292	-0.1286	-0.1237	-0.0805	0.539	0.211
T_Fy <sub>min</sub>	0.2258	0.5714	0.1207	0.2857	-0.434	-0.406
Fy <sub>mean</sub>	-0.1504	0.0948	-0.0384	0.0660	4.411	-3.779
Fy [1/sec]	0.2769	0.2621	0.0842	0.2377	0.027	-0.477
Fx <sub>max</sub>	0.0493	0.1102	0.1040	0.1944	-0.381	-0.303
Fx <sub>min</sub>	-0.0462	-0.0610	0.0231	0.0163	-0.138	0.175
Fx <sub>mean</sub>	-0.0005	0.0201	0.0661	0.1093	-1.048	-0.246
FyP	0.0829	0.0111	0.0188	0.0029		
FyB	-0.1936	-0.0440	-0.7466	-0.1794		
NP	5	6	22	23		
NB	27	53	7	13		
NPB	5	2	5	1		

In an effort to rank the 20 *LPs* and 15 Symmetry factors, we examined the effectiveness of each individual parameter, to classify correctly the rats into the SOD1-G93A mutant and control groups. Using previous modeling experience, we transformed the *LPs* by following the procedures introduced in Liu *et al.* (2008), and Neerchal and Tasch (2008). The misclassification rate improved remarkably when transformed *LP* (*TLP*) was used (see Table 3.3). Therefore, we explored the idea of transforming the *LP* variables using nonlinear transformations (*TLP*) to improve the prediction performance of the model. One such family of nonlinear transformations is obtained by expanding each *LP* in terms of a spline basis (Schumaker, 2007). The misclassification performance of each individual *TLP* ranged from 18.4 to 39.9%, where *FyB* had the best performance, and the Symmetry factor of the Stride (*Sym\_Stride*) had the worst (see Table 3.3).

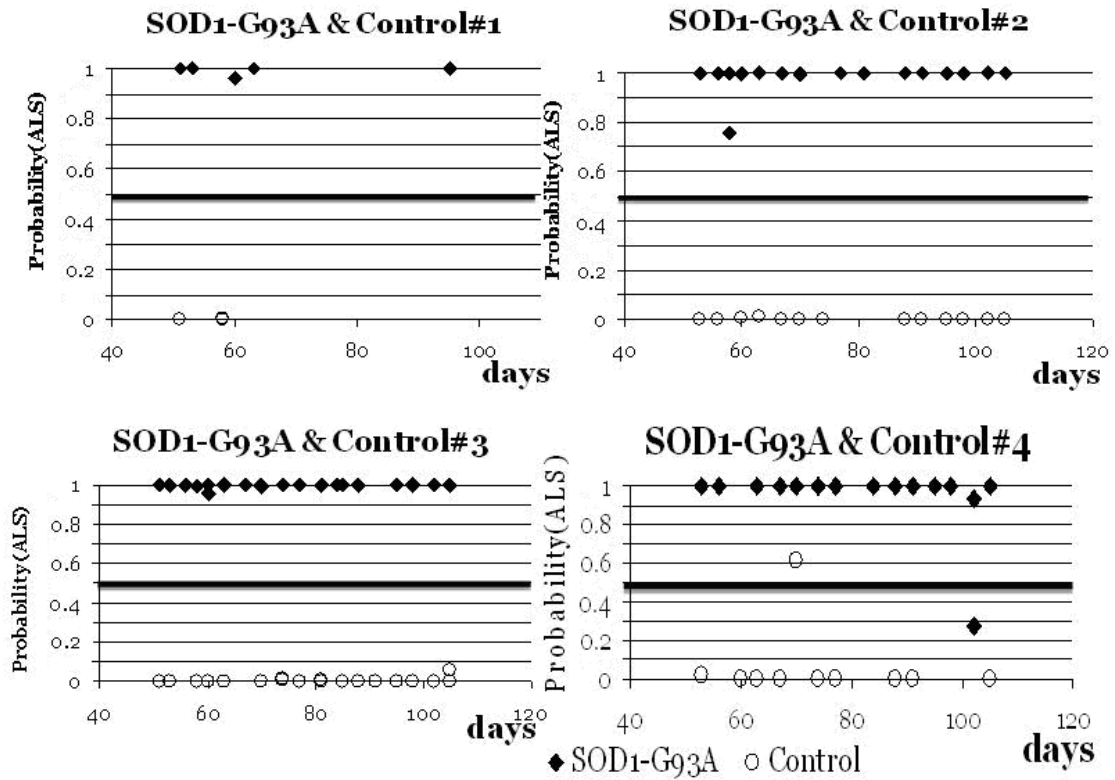
Lastly, when the logistic regression model is based on the transformed values of the top 7 variables listed in Table 3.3 (*FyB*, *T\_Fymax*, *Fymax*, *Fzw*, *Fzmean*, *Fyw*, and *NP*), the range of probabilities that a control rat belongs to the SOD1-G93A mutant group is from 0.000 to 0.002, and the range of probabilities that an SOD1-G93A mutant belongs to the SOD1 group is from 0.998 to 1.000 (see Figure 3.1). Hence, the 7-variable model has no overlap between the SOD1-G93A mutant and the control groups, and its performance turns out to be excellent from the very first test run of the 4 SOD1-G93A mutants and 4 control SD rats (see Figure 3.2).

Table 3.3 Misclassification rates, in percentage, obtained by using a single *LP* or its associated transform *TLP*.

<b>Locomotion Parameter <i>LP</i></b>	<b>Misclassification Rate of <i>LP</i> (%)</b>	<b>Misclassification rate of <i>TLP</i>(%)</b>
FyB	34.0	18.4
T Fy <sub>max</sub>	33.1	20.3
Fy <sub>max</sub>	40.5	24.5
Fz	41.7	25.2
Fz <sub>mean</sub>	40.5	25.8
Fy	37.4	25.8
NP	38.6	25.8
Fx <sub>max</sub>	41.7	25.8
Fz <sub>max</sub>	42.3	26.4
FyP	41.2	26.4
T Fy <sub>min</sub>	39.3	27.0
Stance time	36.2	27.6
Fy <sub>min</sub>	38.7	27.6
Fy <sub>mean</sub>	36.8	27.6
Stride	40.5	28.2
Fx <sub>mean</sub>	36.6	28.2
NB	38.6	28.2
Sym Fx <sub>min</sub>	41.1	28.8
T Fz <sub>max</sub>	40.5	28.8
Sym T Fy <sub>max</sub>	41.3	29.5
Sym Fx <sub>max</sub>	41.7	31.9
Sym Stance time	38.0	32.5
Fx <sub>min</sub>	42.3	32.5
Fy	40.5	33.1
Sym T Fz <sub>max</sub>	41.5	33.7
Sym Fy <sub>max</sub>	41.1	33.7
NPB	41.8	33.7
Sym Fz <sub>mean</sub>	37.4	34.4
Sym Fz <sub>max</sub>	42.3	35.0
Sym T Fy <sub>min</sub>	42.0	35.0
Sym Fy <sub>mean</sub>	40.5	35.0
Sym Fz	36.4	35.6
Sym Fx <sub>mean</sub>	38.7	35.6
Sym Fy <sub>min</sub>	42.0	38.7
Sym Stride	41.7	39.9



**Figure 3.1** The range of predicting probabilities that the examined rat belongs to the SOD1-G93A group. Note large spread and big overlap between the control and SOD1-G93A groups when 1 Variable is used. When 4 Variables are used the overlap between the two groups shrinks a little, nevertheless when a 7-variable model is used there is an almost complete separation between the control and the SOD1 groups. This separation enables us to classify the rats correctly in each and every test run.



**Figure 3.2** Probability of ALS for 4 SOD1 and 4 control rats vs. days for the animals that traversed through the noninvasive diagnostic system. Note that P (ALS) for SOD1 and control rats are close to 1.0 and 0.0, respectively, in all days except for a single day for rat #4.

### 3.4 Discussion of the ALS Experiment

This chapter demonstrates that a logistic regression model with the “proper” explanatory locomotion variables can differentiate between SOD1-G93A mutant and control SD rats from the very first time the examined rats cross a locomotion analysis system, and the resultant classification is excellent. The ability to detect neurological diseases early will allow researchers to test intervention therapies and hopefully to find cures to serious diseases that currently incurable.

The selection of the number of locomotion parameters (*LPs*) used to construct a logistic regression model was based on the misclassification performance of each individual variable. Since the misclassification rate of the eighth variable is 25.8% which is the same as the values of the fifth through the seventh variables (see Table 3.3), we cannot justify the discrimination against the eighth variable ( $Fx_{max}$ ). Nevertheless, from an engineering point of view, the measurements of 8 *LPs* require 14 load cells, whereas 7 *LPs* require only 10 load cells, which are preferred from system cost considerations.

Sweets (condensed milk) and individual cylindrical toys that are placed at the exit platform were used to encourage the rats, in the current system design, to walk through the system. Rats walk through the system at their own pace and will. This explains the discrepancies in the number of test runs for different rats. It is apparent that rats #102 and #106 do not walk as often as their test mates rats #103, #104, #105, #107, #108, or #109 (see Figures 3.2).

In this chapter we examined 4 SOD1-G93A mutant and 4 SD control rats. Obviously, the database consists of several repeated observations. It is well known that repeated observations from the same rat may be correlated. Correlated observations usually do not affect the predictions adversely, but they cause the corresponding prediction errors to be under-estimated. The current study demonstrates the feasibility of the approach however a much larger study with larger number of rats is needed. We plan to use the results of this chapter as a basis for a power study to investigate sample size issues. Obviously, one needs to repeat the experiments with larger populations. Nevertheless, the analysis presented here is not based on visualization of gait abnormalities, as all the SOD1-G93A animals were pre-symptomatic. It has been demonstrated that the earliest change in locomotion is at the neuromuscular junction where there is a process of denervation and re-innervation occurring before any changes in the number of lower motor space neurons have occurred (Fischer *et al.*, 2004).

It can be hypothesized that various other neurological diseases that affect gait, such as Parkinson, Huntington, and Multiple Sclerosis, could also be detected in laboratory animal models using the same methodology. The key will be to find the “proper” *LPs* that constitute biomarkers of the disease one investigates. Furthermore, various pattern recognition strategies can be employed to develop diagnostic tools for other neurological diseases.

## Chapter 4: Gait Analysis of Locomotory Impairment in Rats Before and After Neuromuscular Injury

### 4.1 Introduction to the Locomotory Impairment

We used GAS described in chapter 2 to measure the changes in locomotion parameters of adult Sprague-Dawley rats after neuromuscular injury, induced by repeated large strain lengthening contractions of the dorsiflexors muscles. We developed a logistic regression model from test runs of control and permanently impaired (denervation of the dorsiflexor muscles) rats and used this model to predict the probabilities of locomotory impairment in rats injured by lengthening contractions. The data showed that GAS predicts the probability of locomotory impairment with very high reliability, with values close to 100% immediately after injury and close to 0% after several weeks of recovery from injury. The 6 transformed locomotion parameters most effective in the model were in 3 domains: frequency, force, and time. We conclude that application of the GAS instrument with our predictive model accurately identifies locomotory changes due to neuromuscular deficits. Use of this technology should be valuable for monitoring the progression of a neuromuscular disease and the effects of therapeutic interventions.

Rats and mice have become increasingly important for modeling human diseases and have provided many insights into pathogenic mechanisms (Durbeej and Campbell, 2002), but assessment of the phenotypic changes in rodent models is sometimes difficult. In many cases, severe measures, often involving terminal experiments, are required to detect phenotypical changes including harvesting of tissue to assess



histological changes or for in vitro studies (DelloRusso *et al.*, 2001; Durbeej and Campbell, 2002; Hamer *et al.*, 2002). Since many diseases of the nervous and musculoskeletal systems result in impaired locomotion, non-invasive measurement of locomotion parameters (*LP*) could provide new insights into these diseases as well as facilitating longitudinal studies of their progression and treatment.

We have described a system that uses load cells and video technology to assess quantitatively the gait of rats. The GAS (Tasch *et al.*, 2008) is capable of measuring 20 different parameters of locomotion and provides a non-invasive measure of locomotion in individual rats over time. The sketch of GAS is shown in Figure 4.1. We recently used it to distinguish differences in gait between control and SOD1-G93A rats, a model of amyotrophic lateral sclerosis in man, at pre-symptomatic stages (Tang *et al.*, 2009b). Here we test the hypothesis that our quantitative measurements can detect changes in gait that are induced by permanent impairment of function of a single lower hind limb, and further, that it can detect subtle changes in gait, linked to the partial and temporary loss of muscle function.

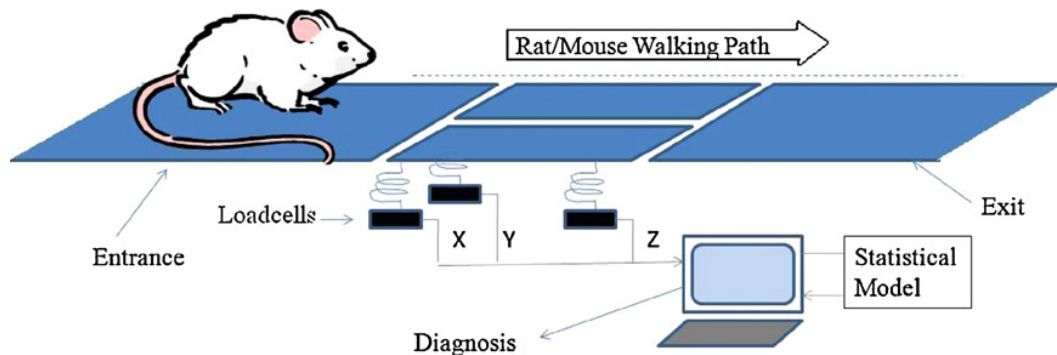


**Figure 4.1** A schematic of the gait analysis system for rodents. The system measures locomotion parameters in 4 domains: force, space, time and frequency. The measured forces are in vertical (*Z*), longitudinal (*Y*) and transverse (*X*) directions. The locomotion parameters feed a statistical model that calculates the probability that a rodent displays locomotion impairment.

## 4.2 Methods and Materials

### 4.2.1 Associating Segments of Load cell Signals and Limbs

Figure 4.2 shows load cell signals during the time period of 0.63 to 0.79 s generated when the RF limb is in contact with the right floor plate. We can associate the other limbs with the signals from the load cell signals that they generate similarly. By designating each fore and hind limb with dashed and solid lines, respectively (Figure 4.3), we can calculate numerous *LPs* that characterize the locomotion of a rat through each limb for every test run.

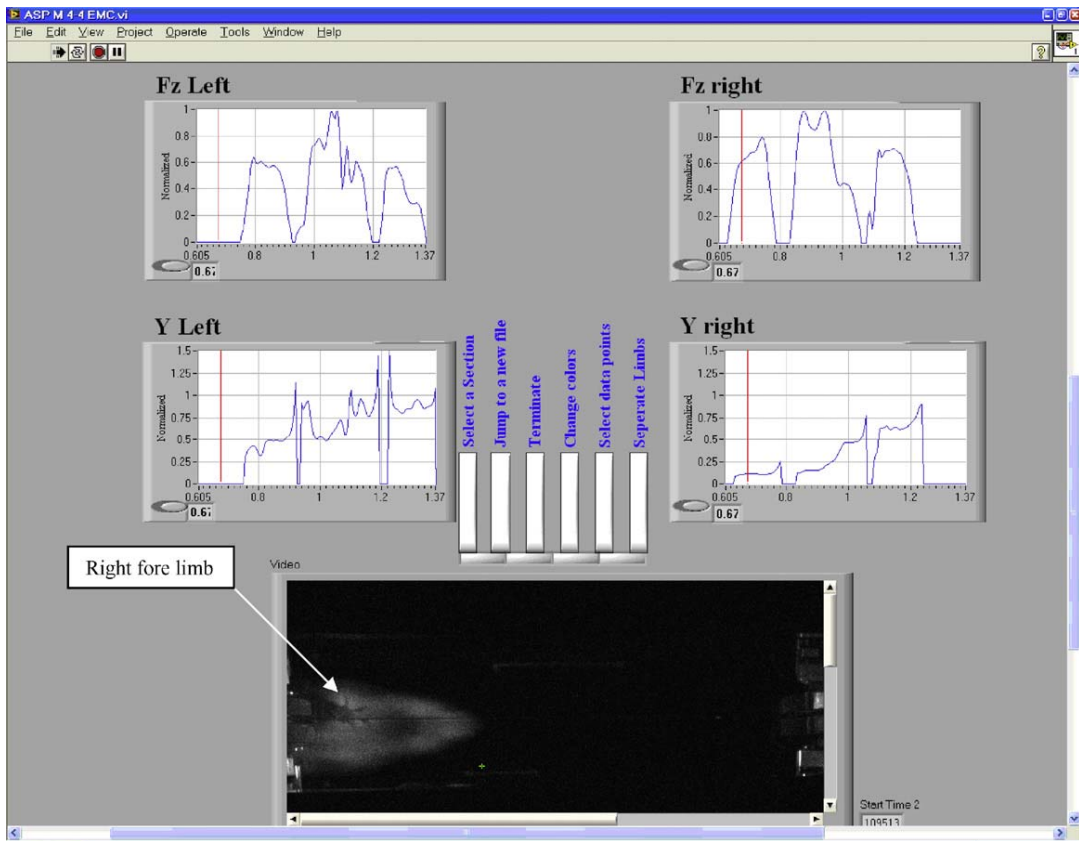


**Figure 4.2** To associate load cell signatures with a limb the computer mouse is placed on a selected signature (vertical red marker) and the most recent video image is displayed. The load cell signature on the right floor-plate from 0.63 to 0.79 s is associated with the right fore limb.

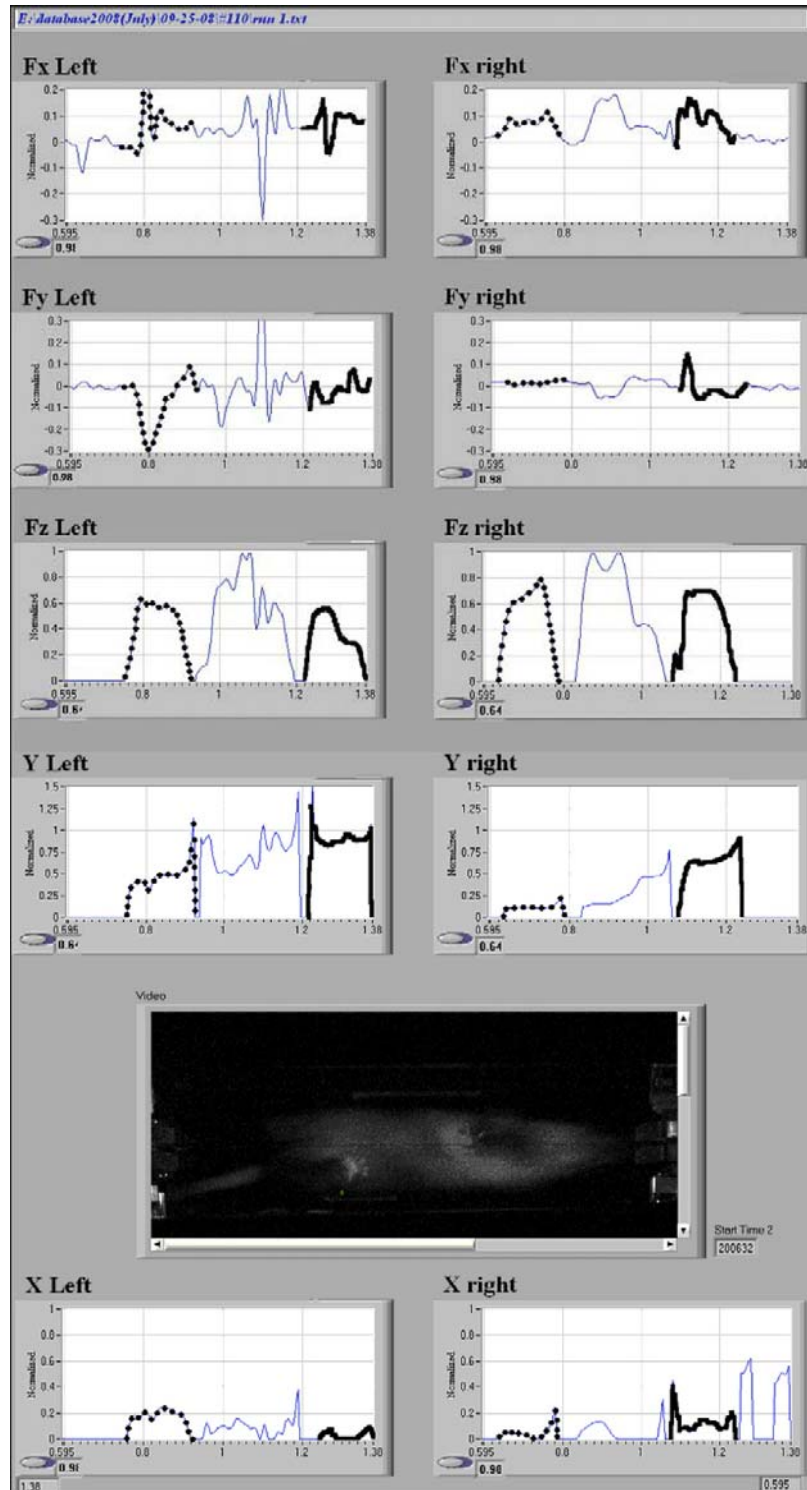


**Figure 4.3** The load signatures generated by a single limb are identified and the fore and hind limbs are marked with dashed and solid heavy lines, respectively.

#### 4.2.2 Obtain Gait Measurements for the Locomotory Impairment Experiment

Ten male, Sprague-Dawley rats (46 days old) from Charles River Laboratories (Shrewsbury, MA) were used in the study. Each rat was housed in a separate cage with darkness/lighting cycle, 12 hours on and 12 hours off, and food and water *ad libitum*. The animals were weighed and placed individually at the system entrance (Figure 4.1). Upon opening of the gate, the rat crossed the system, moving towards its toy and food, placed at the system's exit. This procedure was repeated up to 3 times for each rat on a single day. After 7 days of training and adaptation to the system, each animal was tested twice per week. Data were recorded when the rats reached 55 days of age and for the next 87 consecutive days.

Permanent neuromuscular damage was introduced to the left hind limb in 5 of the 10 rats, at the age of 102 days, while the biweekly data recording continued. The procedure consisted of cutting the fibular nerve, which innervates the dorsiflexors muscles and is easily accessible due to its subcutaneous location at the neck of the fibula (lateral knee). Under sterile conditions, the skin was shaved, a small (less than 1.5 cm) incision was made, and the nerve was identified and cut. To ensure that nerve growth did not ensue, we removed a small section (~5 mm) of the nerve. The incision was sutured closed and topical antibiotics and analgesics were applied. A record of 264 test runs (112 test runs of rats with permanent locomotory impairment, and 152 test runs of control rats) established the training database that we used to derive the logistic regression model for rats with locomotory impairment.

Transient neuromuscular injury was introduced to the left hind limbs at 172 days of age in 3 of the 5 remaining rats, used previously as controls, by inducing 8 large-

strain lengthening contractions to the ankle dorsiflexor muscles based on methods previously described, with some modifications (Lovering *et al.*, 2007). This protocol resulted in a  $44 \pm 6\%$  loss of maximal isometric tetanic torque in the dorsiflexors muscles immediately after injury. To compare pre and post-injury locomotion, we recorded data from one week prior to injury through 5 weeks after injury. A total of 123 test runs were recorded to establish the testing database, which we used to assess the severity of locomotory impairment of the injured rats.

#### 4.2.3 Assessing the Severity of Locomotory Impairment

The logistic regression model obtained for control rats and rats with permanent neuromuscular damage (denervation) was applied to test the locomotion of rats that sustained a transient impairment of muscle function caused by lengthening contractions. Using the probability value, we were able to identify deterioration of locomotion after the transient injury, as well as improvement during recovery from the injury.

### 4.3 Results of the Locomotory Experiment

We used the GAS system (Tasch *et al.*, 2008) to measure 20 different parameters of the gait of walking rats, and present vertical ( $Fz$ ), longitudinal ( $Fy$ ), and transverse ( $Fx$ ) components of the ground reaction forces (GRF), as well as longitudinal ( $Y$ ) and transverse ( $X$ ) limb positions, plotted versus time ( $s$ ) for both left and right floor plates, in Figure 4.1. We used images of the walking rat, recorded from below by a video camera, to associate particular signals generated by the system with the position and activity of individual limbs. Each fore and hind limb is designated with dashed

and solid lines, respectively (Figure 4.3), enabling us to calculate the locomotion parameters (*LPs*) associated with the movements of individual limbs for every test run.

Table 2.1 lists the 20 *LPs* that we evaluated for every limb, for every test run of control and permanently impaired (denervated) rats. The numerical values of *LPs*, recorded for a permanently impaired rat and for a control rat, are presented in Table 4.1. Note the generally lower *LP* force values of the LH limb, which had been denervated by fibular nerve section 12 days prior to the test.

Table 4.1 Numerical values of the 20 measured *LPs* for a permanently impaired and control rats. Data of the permanently impaired rat were recorded when the denervated rat was 114 days old and 12 days after introducing the permanent locomotory impairment. Data of the control rat, recorded at 94 days of age. Note the generally reduced force capacity of the LH limb of the denervated rat. Except for stance time,  $F_z$  and  $F_y$ , all other variables are non dimensional.

Locomotion Parameter (LP)	Denervated rat – 12 days after being introduced to a permanent locomotory impairment				Control rat			
	LF	RF	LH	RH	LF	RF	LH	RH
$F_{z_{max}}$	0.6330	0.6316	0.3628	0.8133	0.7263	0.6801	0.4944	0.5138
Stance time [s]	0.1500	0.1650	0.1750	0.3050	0.2950	0.3000	0.8650	0.4350
$T_{F_{z_{max}}}$	0.4000	0.3939	0.3143	0.2295	0.3220	0.2667	0.7052	0.1609
$F_{z_{mean}}$	0.4015	0.4163	0.2161	0.4614	0.3722	0.4157	0.3541	0.4008
$F_z \cdot [1/s]$	0.3946	0.4117	0.2452	0.6158	0.6051	0.6505	0.3941	0.3876
Stride	0.4927	0.6649	0.4582	0.5608	0.2381	0.4114	0.0669	0.0676
$F_{y_{max}}$	0.0631	0.0405	0.0555	-0.0050	0.2079	0.3047	0.2303	0.1440
$T_{F_{y_{max}}}$	0.9000	0.6970	0.6857	0.0492	0.3729	0.9500	0.7168	0.0345
$F_{y_{min}}$	-0.1906	-0.0012	-0.1433	-0.3142	-0.3030	-0.3995	-0.0887	0.0283
$T_{F_{y_{min}}}$	0.2333	0	0.0286	0.2787	0.4576	0.3000	0.9653	1.0000
$F_{y_{mean}}$	-0.0490	0.0232	-0.0351	-0.0668	0.0046	-0.0180	0.0233	0.0823
$F_y \cdot [1/s]$	0.1127	0.0247	0.0953	0.1758	0.2529	0.2345	0.0822	0.1084
$F_{x_{max}}$	0.0010	0.1322	0.0192	0.1925	0.2225	0.1779	0.0421	0.1726
$F_{x_{min}}$	-0.0892	-0.0150	-0.0534	-0.0025	-0.2698	-0.1282	-0.1132	0.0444
$F_{x_{mean}}$	-0.0001	0.0626	0.0006	0.0913	0.0156	0.0691	0.0079	0.1180
$F_{yP}$	0.0375	0.0152	0.0338	0	0.1058	0.0956	0.0502	0.0685
$F_{yB}$	-0.1115	-1.0030	-0.0548	-0.0248	-0.0841	-0.0897	-0.0367	0.0000
NP	13	32	8	0	28	31	120	88
NB	18	2	28	62	32	30	54	0
NPB	6	1	2	0	10	3	14	0

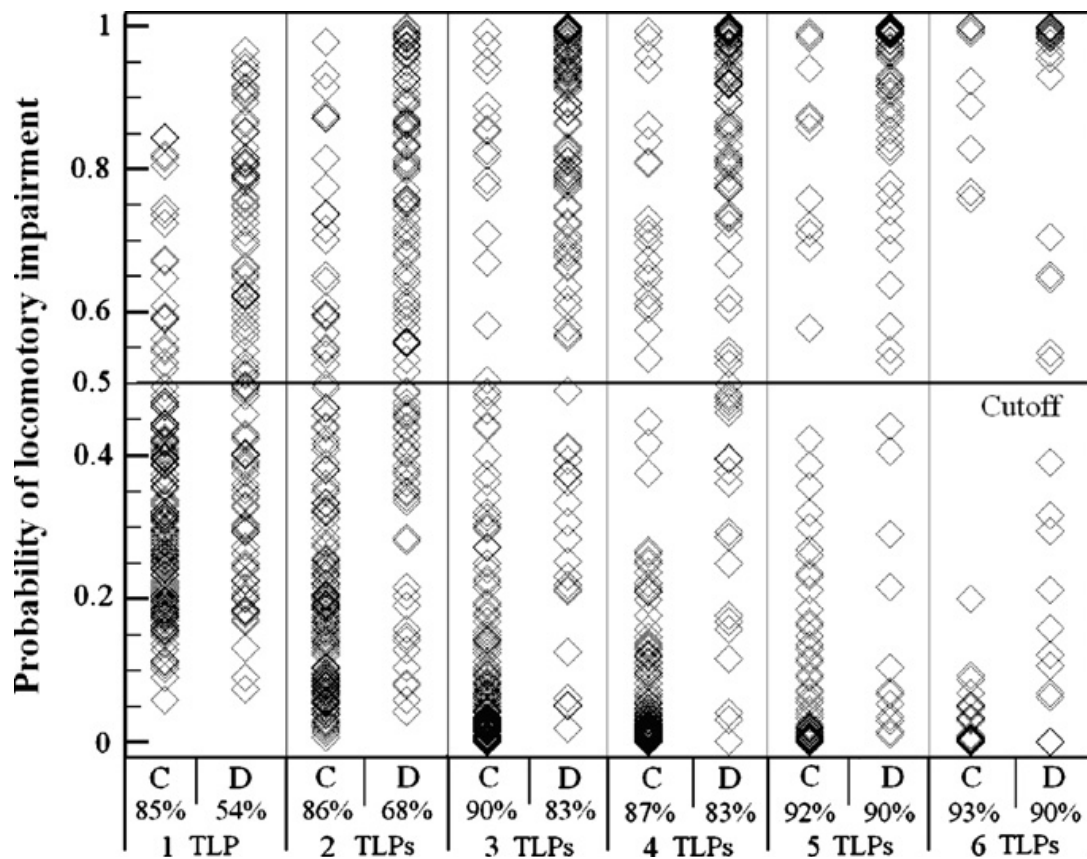
In an effort to rank the effectiveness of the 20 *LPs* in detecting defects in locomotion, we examined the effectiveness of each individual *LP* to classify the rats correctly into permanently impaired and control groups. We transformed the *LPs* by following the procedures introduced in Liu *et al.* (2009). The classification rate improved remarkably when the *LPs* were transformed using spline transformation (Schumaker, 2007), such that the probability of misclassification by the model when the top 6 individual transformed *LPs* (*TLPs*) were used, ranged from 26.5% to 28.8%. Table 4.2 prioritizes the 6 most useful *TLPs*, one *TLP* at a time.  $Fz\omega$  was the best predictor; and the propulsion duration period (NP) was the worst.

Table 4.2 Ranking the transformed *LPs* based on their misclassification performance when a single *TLP* is used at a time. The misclassification rate of the Fourier transform of the vertical reaction force,  $Fz\omega$ , is the best with misclassification rate of 26.5%, and the time duration during which the longitudinal reaction is propelling, NP, has the worst performance with misclassification rate of 28.8%.

<b>TLP</b>	<b>Misclassification [%]</b>
$Fz\omega$	26.5
$Fy_{\text{mean}}$	26.9
$Fx_{\text{min}}$	28.0
NB	28.0
$Fz_{\text{mean}}$	28.4
NP	28.8

When we derived a logistic regression model based on the transformed values of the best 1 to 6 *TLPs* listed in Table 4.2, our ability to identify control versus denervated animals from the data alone improved with the number of these variables that we used (Figure 4.4). The cutoff value of the probability predictions for the control and denervated groups was 0.5. Incorporating a total of 6 variables into the model and selecting a probability cutoff value of 0.5 provide specificity and sensitivity exceeding 90% in analyses of control and denervated rats (Figure 4.4).





**Figure 4.4** The range of predicting probabilities that the examined rat has locomotory impairment when 1, 2, 3. . . and 6 top performing *TLPs* (listed in Table 4.2) are used. C is control and D is denervated or permanently impaired groups. The cutoff value of the probability predictions for the control and denervated groups was 0.5. Note the improved specificity and sensitivity of the control (C) and denervated (D) groups, as the number of *TLPs* increases from 1 to 6.

We used the 6-variable model of control and permanently impaired rats to calculate the probability of impairment in the locomotion of 3 rats (Figure 4.5), injured by a series of large strain lengthening contractions of their ankle dorsiflexors in one hind limb. Our functional measurements indicate that the ankle dorsiflexors lose ~ 45% of the contractile torque after this form of injury (Lovering *et al.*, 2007). Prior to injury, all of the rats demonstrated a probability of impairment in locomotion of less than 0.5 (Figure 4.5). Immediately after injury, all 3 injured rats showed a probability of impairment in locomotion of about 1. Furthermore, our analysis of

probabilities indicated that all 3 rats recovered fully, i.e., their probabilities of impairment approached 0 over time, although at different rates (6, 20, and 34 days for complete recovery). We conclude that the 6 *LPs*, determined by our apparatus and subjected to spline transformation, can reliably identify rats that have been subjected to an injury that partially reduces the efficacy of only one muscle group (the ankle dorsiflexors) in a single hind limb.

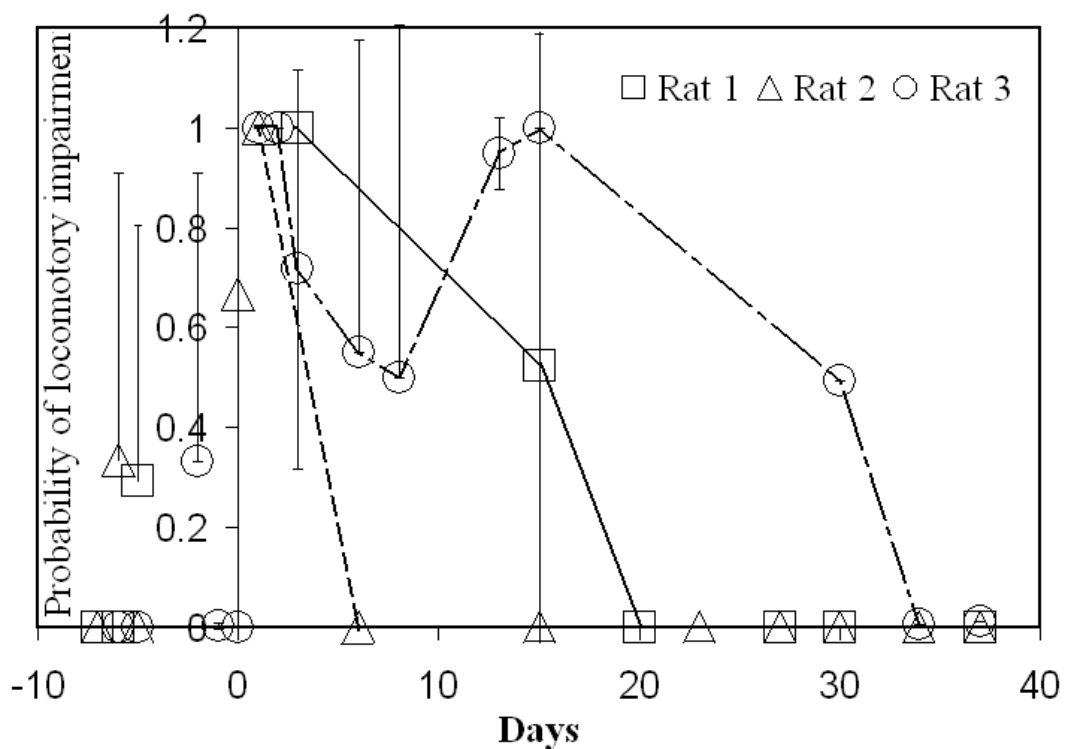


**Figure 4.5** The probability of locomotory impairment of the three injured rats. Large strain injury was induced on day 0. The alteration in gait after injury is reflected by the high probability of locomotion impairment at day 0. Despite, animal to animal variability in gait during the 5 weeks after injury, the probability of locomotion impairment for all three animals returned to pre-injury levels by the 34<sup>th</sup> day. The cutoff value of the probability predictions for locomotory impairment was 0.5. The vertical bars are the error bars.

#### 4.4 Discussion of the Locomotory Experiment

Analysis of locomotion in rodents can be useful in assessing normal or altered neuromuscular function (Clarke, 1991). Measurements of the ground forces applied by the limbs during locomotion provide a non-invasive way to assess gait and monitor functions of individual limbs in locomoting rats (Muir and Whishaw, 1999). Rats with lesions similar to those seen in Huntington's disease show spontaneous motor symptoms that include gait abnormalities (Guvot, *et al.*, 1979). These abnormalities are not easily detected by eye, but were readily identified and quantified by computerized video analysis. Quantitative methods to assess temporal and spatial locomotion parameters have been reported (Hamers *et al.*, 2001). Non-quantitative video-based methods to characterize the effects of nerve injury are also available (Walker *et al.*, 1994). These methods assess multiple locomotion parameters, but the data they produce have not been used to determine whether a certain type of disease or locomotion impairment is present. The GAS records locomotion parameters, associates the signals with the placement of individual limbs, and assesses the probability that certain locomotion impairment is present. Here we use the GAS to establish the parameters associated with gait abnormalities caused by denervation of a single limb and to assess, with a high degree of reliability, changes in gait that are linked to much milder and reversible injuries.

Our results show that GAS is an effective tool for evaluating permanent or temporary defects in gait consequent to neuromuscular injury. To develop a model that could be used effectively to identify changes in gait associated with mild and reversible injuries; we first prepared a dataset from rats that we trained to walk

through the GAS system. Comparisons of locomotion records of control rats and rats with permanent locomotory impairment, caused by denervation of a single hind limb, revealed clear differences. After analyzing these differences using spline transformation, we generated datasets that we then applied to examine the effects of injuries caused by several large-strain lengthening contractions in a single hind limb. In particular, we selected 6 parameters from this dataset that were most effective in identifying denervated and control rats, which we then applied to the data we obtained from the injured animals.

From this dataset we generated a logistic regression model that predicted the probability of locomotory impairment and reliably identified those animals that had been mildly and reversibly injured by lengthening contractions. We also used these parameters to follow the recovery of gait in individual animals for 5 weeks after injury. The ability of the GAS to identify injured animals and to determine when they have recovered from the injury, which causes only a ~ 45% loss of function of a single group of muscles in one hind limb, suggests that the instrument and the analytic methods we have developed are both highly sensitive and reliable.

Interestingly, despite using an injury model that produces a stereotypical response in terms of loss and recovery of contractile torque (Lovering *et al.*, 2007), each animal that we tested with the GAS showed a unique time course for recovery of gait. This suggests that, similar to humans, factors such as pain and the ability to compensate for injury may affect gait in rats. Future studies with the GAS will test if therapeutic interventions that reduce pain and inflammation improve gait during the days that follow injury from lengthening contractions.

## Chapter 5: Locomotion Analysis of Sprague-Dawley Rats Before and After Injecting 6-OHDA

### 5.1 Introduction to the Parkinsonian Models

This chapter focuses on distinguishing the locomotion of 6-OH dopamine (6-OHDA) rats from untreated control rats. A 6-OHDA rat is a model of Parkinson's disease and the locomotion is determined by measuring ground reaction forces. This chapter tests the hypothesis that changes in measured locomotion parameters can noninvasively detect Parkinson's disease in rats.

A gait analysis system that measures locomotion parameters of each individual limb along with a logistic regression model are used to assess the locomotion impairments of Sprague-Dawley rats before and after injecting 6-OHDA into their right medial forebrain bundle. The statistical model used 7 locomotion parameters that characterize non vertical ground reaction forces and associated time parameters.

We observed changes in the rats' locomotion as soon as they walked again through the system after recuperating from the surgery. Before the surgery, the locomotion of the rats was not impaired, whereas after surgery the six rats demonstrated impaired locomotion. The sensitivity and specificity of the 7 locomotion parameters model is 92% and 95%, respectively. This model calculated the predicting probabilities that Parkinson is present prior to and after the injection of 6-OHDA to be less than 0.34 and more than 0.67, respectively.

Parkinson's disease and other neurological ailments that affect locomotion can be detected by measuring locomotion parameters that are based on ground reaction

forces. The severity of locomotion disorders due to genetic diseases (SOD1-G93A rat model of Amyotrophic Lateral Sclerosis), neurotoxin-induced diseases (6-OHDA rat model of Parkinson), and injury-induced diseases is compared.

It has been recently reported that a computerized gait analysis system is unable to consistently identify motor problems in MPTP-treated mice, a model of Parkinson's disease (PD), despite a 90% deficit of striatal dopamine content (Guillot *et al.*, 2008). In addition it was also found that the same gait analysis system could not distinguish SOD1-G93A, a mouse model of ALS, from controls, up to 84 days of age. This contradicts our findings (Tang *et al.*, 2009a) where SOD1-G93A rats were distinguished from Sprague-Dawley (SD) non-transgenic controls, as early as at 51 days of age, with sensitivity and specificity of 98% and 99%, respectively. The contradiction between the two reports is resolved by paying attention to the two distinct gait analysis systems used in the studies. Guillot's study used a computerized treadmill system that utilizes video technology to record multiple locomotion parameters (*LPs*) in the space and time domains; whereas Tang's study used a system that utilizes load cells to records multiple *LPs* of each individual limb in space, time, force, and frequency domains (Tasch *et al.*, 2008). *LPs* in the force and frequency domains were not only crucial for the identification of motor problems in SOD1-G93A, they were also key parameters in denervation studies (Tang *et al.*, 2009b). We sought to determine whether our system of recording and ranking multiple gait parameters based upon the values of *LPs* in four domains would be applicable to another model of PD, the 6-OHDA-lesioned rat.

This chapter focuses on distinguishing the locomotion as determined by the measurement of ground reaction forces between, 6-OHDA rats, a model of PD, and untreated control rats. It was reported (Amende *et al.*, 2005) that the stride length was significantly shorter and stride frequency was significantly higher in methyl-phenyl-tetrahydro-pyridine (MPTP) treated mice (a mouse model of Parkinson's disease) when compared to the values obtained from a control mouse. In another study (Metz *et al.*, 2005) found that 6-OHDA rats showed a shuffling gait and short stride lengths but in a straight walk, the lesioned animals had normal coupled hindlimb stepping.

Sudden turns during walking were reported to be impaired in people with Parkinson's disease (Mak *et al.*, 2005), and in another study (Plotnik *et al.*, 2008) stated that freezing of gait, in patients with Parkinson's disease, occurs most frequently during turns or step initiation. This was also seen in 6-OHDA-lesioned animals (Metz *et al.*, 2005). Sudden turns and step initiation are two tasks that demand a high degree of bilateral coordination between the legs (Plotnik *et al.*, 2008), nevertheless these tasks also require moderation of ground reaction forces (GRF) define that is being overlooked by many researchers.

## **5.2 Methods and Materials**

### **5.2.1 Animal Experiment and Surgery**

Six adult Sprague-Dawley male rats from Taconic Laboratories, USA were used in the study. Each rat was housed individually with dark/light cycle, 12 hours/12 hours, and food and water ad libitum. All animals were treated in accordance institutional and federal guidelines. We ran each rat in the gait analysis system up to 3 times on a single day, twice per week, after 7 days of training and adaptation to the

system. Data were recorded for 30 days for the six rats (10 days before the injection of 6-OHDA and 20 days after injection). Rats underwent surgery in which 6-OHDA was injected into the right medial forebrain bundle (MFB), following the procedure documented in Muir and Wishaw (1999).

### 5.2.2 Obtain Gait Measurements for the Parkinsonian Experiment

The animals transverse through the gait analysis system before the surgery and 3 days after recovering from the surgery. This protocol was repeated twice per week before and after the surgery. A record of 112 test runs of the 6-OHDA rats and 152 test runs from control rats established the training database (264 test runs totally) that we used to derive the logistic regression model for the 6-OHDA rats. A record of 45 test runs before the surgery and 112 test runs after surgery established the database we used for testing the 6-OHDA model. The 7 *LPs* selected to derive the 6-OHDA model are listed in Table 5.1. At the end of our experiments, animals were euthanized by sodium pentobarbitol injection (150 mg/kg IP) and perfused with paraformaldehyde (4%) for histological analysis.

Table 5.1 The seven *LPs* that best distinguish the locomotion of 6-OHDA from controls, along with their definitions and misclassification rates.

<b>LP</b>	<b>Misclassification Rate [%]</b>
Fymin	23.5
NP	24.6
Fxmax	24.6
Fymean	25.4
Sym_FyP	28.4
Fymax	29.2
NB	30.3



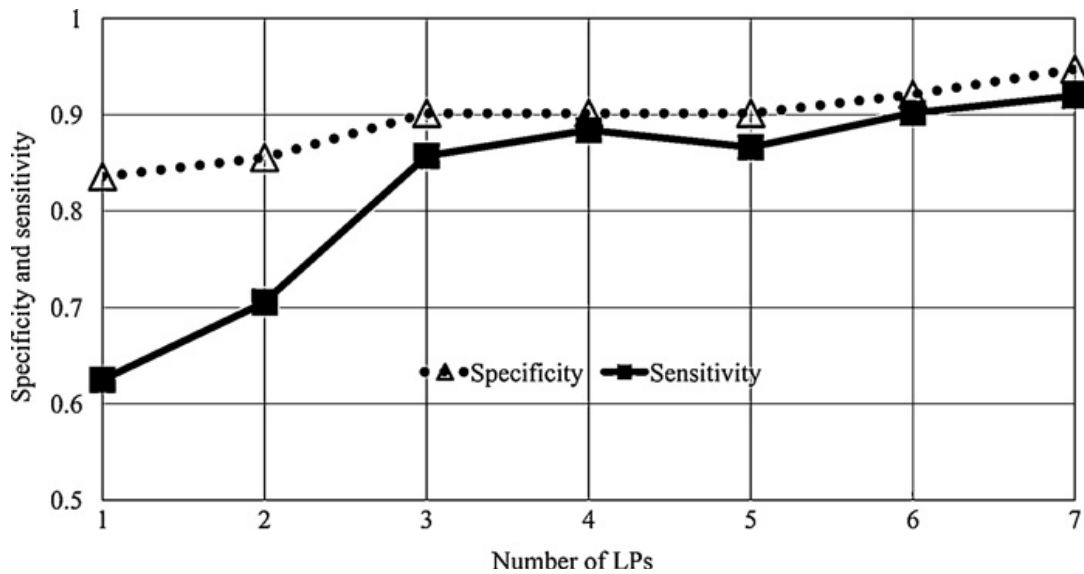
### 5.2.3 Cross Validation of Logistic Regression Model

Leave-One-Out method of cross validation described in Chapter 3 was used to evaluate the performance of the derived 6-OHDA model. A single test run from the original sample was taken as the validation data, and the remaining test runs were taken as the training data. This procedure was repeated 264 times until every test run in the database was used once as the validation data.

### 5.3 Results of the Parkinsonian Experiment

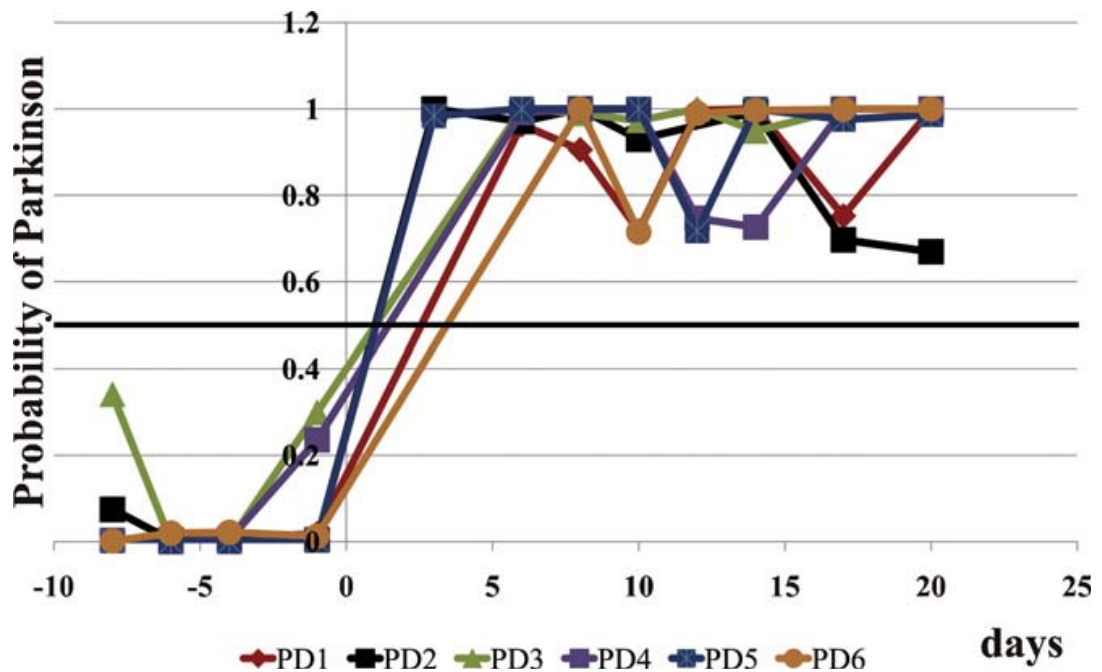
Twenty different *LPs* were recorded as rats walked through a GAS (Tasch *et al.*, 2008). The *LPs* included variables measured in four domains: force, space, time and frequency. These *LPs* were ranked based on their ability to distinguish between the 6-OHDA-lesioned and control rats, similarly to the method introduced in (Tang *et al.*, 2009a). The top seven performing *LPs*, that have the least misclassification errors in distinguishing 6-OHDA from control rats, are listed and defined in Table 5.1. The seven *LPs* are associated with transverse and longitudinal ground reaction forces, as well as propulsion and braking time durations.

Figure 5.1 depicts the specificity and sensitivity values of the model when the top 1, top 2, and up to top 7 *LPs* (listed in Table 5.1) were used. The cutoff probability value was set to 0.5. Note the improved specificity and sensitivity of the 6-OHDA model, from (84%, 63%) to (95%, 92%) as the number of *LPs* increased from 1 to 7.



**Figure. 5.1** Sensitivity and specificity versus the number of best performing locomotion parameters (*LPs*) used to model the locomotion of the 6-OHDA lesioned rats. Best performing *LPs* result in the lowest misclassification errors when the cutoff value is set to 0.5. Note the improved specificity and sensitivity values (0.84–0.95 and 0.63–0.92, respectively) as the number of best performing *LPs* increases from 1 to 7.

The 7-LP model was used to calculate the predicting probabilities in Figure 5.2 ten days prior to, and twenty days following the injection of 6-OHDA into the MFB. Note that prior to the injection the probability that the rats had gait abnormalities was less than 0.34, whereas after the injection (day 0, Figure 5.2) the probability of gait abnormalities similar to Parkinson's disease is mostly 1.0 with a minimum value of 0.67.



**Figure 5.2** The probability that a rat is parkinsonian for the six rats, 10 days prior to and 20 days post-operation. Each data point is an average of minimum two predictions, calculated by the 7-LP model based on leave-one-out method. Note the maximum probability value prior to the 6-OHDA lesion is 0.34, and the minimum probability value after the operation is 0.67.

Table 5.2 The *LPs* that best distinguish between the locomotion of rat models of ALS, Parkinson and muscular injury. Note that different sets of *LPs* are required for distinguishing SOD1-G93A, 6-OHDA, and injured rats from their corresponding controls.

ALS model		Parkinson's disease model		Neuromuscular injury model	
SOD1-G93A	Misclassification Rate of LP[%]	6-OHDA	Misclassification Rate of LP[%]	Muscular Injury	Misclassification Rate of LP[%]
FyB	18.4	Fymin	23.5	Fzw	26.5
T_Fymax	20.3	NP	24.6	Fymean	26.9
Fymax	24.5	Fxmax	24.6	Fxmin	28.0
Fzw	25.2	Fymean	25.4	NB	28.0
Fzmean	25.8	Sym_FyP	28.4	Fzmean	28.4
Fyw	25.8	Fymax	29.2	NP	28.8
NP	25.8	NB	30.3		

Another interesting observation is depicted in Table 5.2. We have used the gait analysis system to derive predictive models of three different diseases:

- (i) Parkinson's disease using the 6-OHDA rat model,
- (ii) neuromuscular injury induced by repeated large-strain lengthening contractions of the dorsiflexor muscles (Tang *et al.*, 2009b), and
- (iii) ALS using the SOD1-G93A rat model (Tang *et al.*, 2009a).

Table 5.2 lists the different sets of top performing LPs that best distinguished between the locomotion of the 6-OHDA, injured, and SOD1-G93A rats to the locomotion of their corresponding controls. Note that each condition has a different set of best performing LPs, which suggests the LPs listed in Table 5.2 to be locomotion biomarkers of 6-OHDA, nerve injured, and SOD1-G93A rats.

#### **5.4 Discussion of the Parkinsonian Experiment**

The seven top performing LPs of the 6-OHDA rats are associated with longitudinal and lateral GRF components only. Variables derived from the vertical GRF component were not included in the model. This is especially relevant to Parkinson's disease since in advanced stages of Parkinson's disease, patients are known to drag or shuffle their feet.

It has been demonstrated in the neuromuscular injury study that the predicted probability decreased as the severity of the injury diminished (Tang *et al.*, 2009b). The current study demonstrated the opposite condition i.e., that the probability of PD increased after introducing the 6-OHDA lesion on day 0. Thus it has been shown that the predicted probability measure reflects the severity level of a disease and it will increase or decrease to reflect the progression of a disease or its recovery.

The LP with the least misclassification rate across the three diseases of ALS, Parkinson, and neuromuscular injury is the braking force (FyB) with a value 18.4% for ALS. Indeed, the specificity and sensitivity of the ALS 7-LP model has the highest values of 98% and 99%, respectively (Tang *et al.*, 2009a). FyB is not a prominent variable in describing gait in either 6-OHDA-lesioned or in neuromuscular injury animals (Tang *et al.*, 2009b). This indicates that there may be differences between gaits in different disorders and/or there may be differences in gait between genetic diseases such as the SOD1-G93A rat (ALS), neurotoxin-induced diseases (6-OHDA rat), or injury-induced diseases.

## Chapter 6: Conclusion and Future Work

### 6.1 Conclusion

This Ph.D. dissertation addresses an effective way to detect neurological and neuromuscular diseases, such as Parkinson's, ALS, and muscular injuries by measuring locomotion parameters in four domains: force, distance, time and frequency. A number of *LPs* are generated from the collected data and several selected *LPs* are used to calculate the probability that a certain disease is present. Different diseases have different sets of effective *LPs* and consequently different sets of statistical models.

Three different statistical models were developed and tested in chapter 3, chapter 4 and chapter 5, respectively. The inputs of the statistical models are some selected *LPs* instead of all *LPs*. The criteria of the *LP* selection are the performance of distinguishing the control group from the treated one. Model performance has two aspects: sensitivity and specificity. In all three developed models both sensitivity and specificity values are better than 90%.

The experiments in this dissertation test the hypothesis that some neurological and neuromuscular diseases which affect gait can be detected at early stages by using gait analysis. There are numbers of modern gait analysis methods which is based on the integration of multiple components to derive a complete analysis of gait. These methods may include observation, videotaping, electromyography, kinematics, kinetics and energetics (Kopf *et al.*, 1998). The method we used in this dissertation is a combination of videotaping, kinematics and energetic.

The main contributions of this Ph.D. dissertation could be concluded as the following:

(a) Three preliminary experiments for ALS, muscular injury and Parkinson's disease were designed and performed, respectively. Tens of thousands of data sets were obtained. The collected gait data could be a valuable reference for the future studies.

(b) An in house gait analysis system for laboratory rats was improved in both software and hardware. The system became to be a movable, reliable and efficient tool for gait analysis study. This work makes the commercialization of the system to be realistic.

(c) A series of statistical methods which can be used to process the locomotion parameters were employed in this dissertation. This work fills in the blank that researchers don't have an effective way to interpret thousands or even millions of gait data sets.

(d) This work developed a method to find a number of significant locomotion parameters which are also called biomarkers. The biomarkers will be used as inputs of the statistical models.

(e) This dissertation tested the hypothesis that the probability is not only a criterion to classify the treated group and the control one, but also a reflection of how severe the disease is. The detail of this contribution is reported in the Chapter 4 of this dissertation.

(f) Training animals is usually important in some animal related experiments. This study reported a way to train the laboratory rats to go through the compartment

without any stops. The condensed milk was used to attract the rats and some toys were introduced.

(g) This dissertation also put effort to develop an efficiency design to calculate a proper sample size we should run in future experiments. The detail of the simulation is attached in the appendix.

There are some deficiencies of this Ph.D. dissertation that will justify future work. For instance, the sample size of the three experiments performed is small. It is obvious that we need a larger sample size. Due to the small sample size, the result we got from the experiments may be too optimistic.

## **6.2 Future Work**

This dissertation reports a methodology to detect neurological and neuromuscular diseases non-invasively. Further research is still required to strengthen and improve our results.

### **6.2.1 Improving the Models by Running Larger Sample Sizes**

A statistical simulation which was performed by Feng *et al.* (2010) shows that a big sample size is needed to get a robust ALS detecting model. Figure 6.1 demonstrates that the classification rate decreases as the number of animals per group increases from 10 to 200. The standard deviation of the classification rate is presented by the vertical bars. One can observe that the classification rate approaches 0.86; the standard deviation decreases as the number of animals increases. Nevertheless, when the number of animals per group is about 50, the classification rate will have already reached a reasonably stable stage.



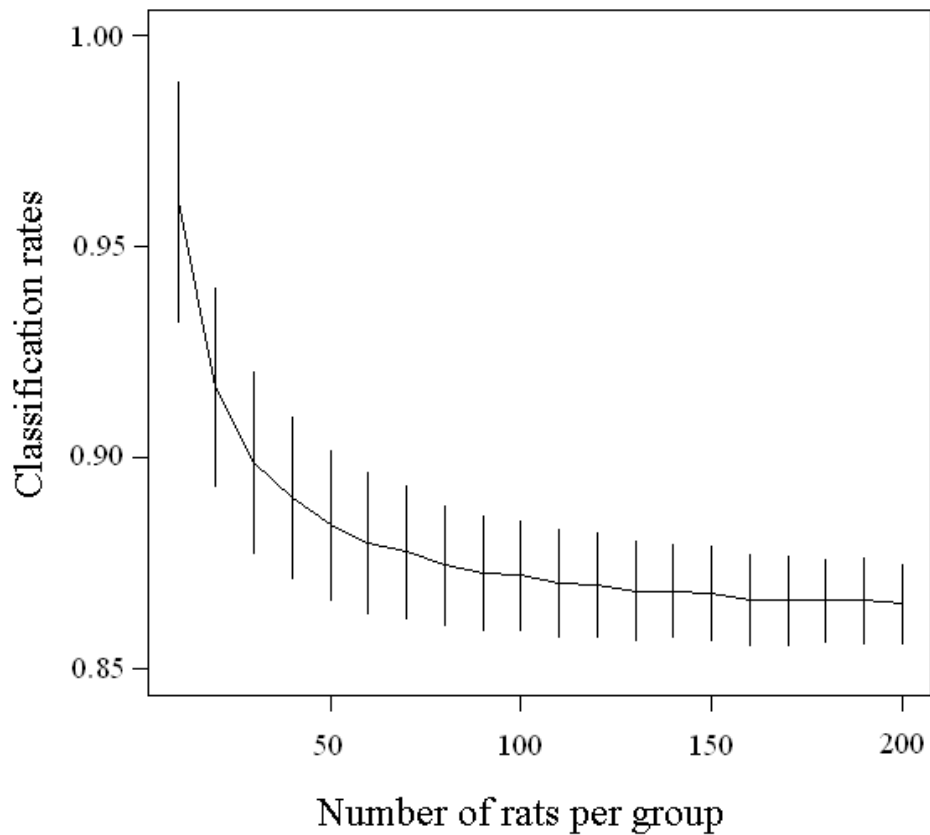


**Figure 6.1** Classification rate versus the number of rats per group for the SOD1-G93A experiment. Vertical lines represent the standard deviation of classification rate.

Figure 6.2 depicts the maximum standard deviation of the coefficients of the logistic regression model divided by the values of the maximum logistic regression coefficient. This standard error is plotted versus number of rats per group. This plot indicates that the maximum standard error is low and stable when the number of rats in each group is 20. We therefore propose to test 50 SOD1-G93A and 50 control SD rats in future ALS experiments.

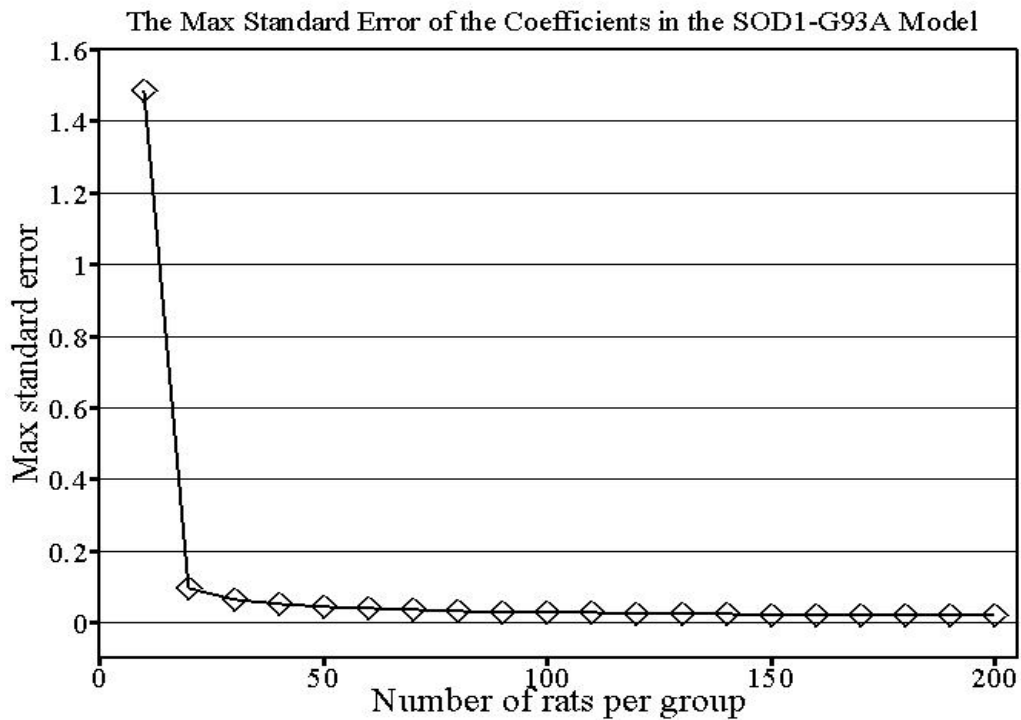


**Figure 6.2** Maximum standard deviation of the coefficients of the logistic regression models for SOD1-G93A laboratory rats.

### 6.2.2 Application of the Methodology to Human

The obvious next step is to investigate the application of the developed methods to humans. It means that we are going to move from four legged species to two legged humans. There are going to be challenges in achieving this goal. In addition to fact that the system has to be adjusted to physical dimension of a human subject, the pressure distribution of the sole may be of great importance and the current system does not measure it. This technically will add many *LPs* that we will have to study and select the most important in capturing the presence of a given disease.

# Appendix: Designing a Study for Developing Predictive Models for Gait Abnormality in Rats

## 1. Introduction

### 1.1. Assessment of Efficient Design

Efforts to model human disease depend heavily on modeling rats and mice. Studying the efficacy of some drugs extensively with animal models often requires using hundreds of animals. If the results are promising, the scientists will advance in the process and begin conducting studies on human subjects. The scientific study of Parkinson's and ALS usually depends specifically on rat models. Niebroj *et al.* (2007) studied the examinations of biochemical and electron microscopic (EM) of the spinal cord myelin from SOD1-G93A rats in both an early and a late symptom-free period of the disease (60 and 93 days of life), and again after four-leg paralysis has occurred (120 days of life). Sexual dimorphism in disease onset was also observed in hSOD1-G93A transgenic rats by Suzuki *et al.* (2007). The disease onset was consistently earlier in male hSOD1-G93A rats. Muir and Whishaw (1999) compared the locomotion of the rats with Parkinson's disease and the control rats by measuring the ground reaction forces.

Each of the studies requires a large number of the laboratory rats. Therefore, the cost of laboratory animals is a major budget concern for any subsequent trials. For instance, an SOD1-G93A rat developed by Jackson *et al.* (2002) and Howland *et al.* (2002) could cost up to \$100.00 each. Furthermore, performing experiments with rats is very labor intensive. Therefore, finding an appropriate sample size becomes the

most crucial part of the trial. In this paper, we investigate both the development of a design and the determination of sample size for the gait analysis experiment. This is a part of an ongoing project at UMBC, where researchers have developed very effective models for diagnosing Amyotrophic Lateral Sclerosis (ALS).

## **1.2 Gait Analysis System**

A gait analysis system (GAS), which is introduced in Tasch *et al.* (2008), can be used to distinguish ALS rats from control rats, as described in Tang *et al.* (2009a), and to detect neurological and neuromuscular diseases, as also reported by Tang *et al.* (2009b). The GAS (see Figure 2.1), which can record video images, measures vertical, longitudinal, and transverse ground reaction force (GRF). Spatial (longitudinal and transverse) limb positions of walking laboratory rats can be observed with the GAS as well.

## **1.3. Locomotion Parameters (LPs)**

Based on the GRF signals and the recorded images captured by the GAS, the values of 20 LPs per limb were evaluated for the left fore (LF), right fore (RF), left hind (LH), and right hind (RH) limbs. These *LP* values were ranked according to their individual abilities to distinguish between the control and SOD1-G93A rats. The LPs with smaller misclassification error have a higher ability of distinguishing SOD1-G93A rats from controls. The 20 *LPs* are listed in Table 1 of Tang *et al.* (2009a).

## **1.4. Logistic Regression Model**

The Logistic regression model is used in Tang *et al.* (2009a) to predict the probability that ALS is present—that is, the model determines that a tested rat belongs

to the SOD1-G93A mutant group. The  $LPs$  were used as the predictors in the logistic regression model:

$$\text{logit}(\pi) = \log \frac{\pi}{1-\pi} = \beta_0 + \sum_{i=1}^k \beta_i \cdot LP_i \quad , \quad (\text{a-1})$$

where  $\pi$  is the probability that a rat belongs to the SOD1 group. Hence

$$\pi = \frac{\exp(\beta_0 + \sum \beta_i \cdot LP_i)}{1 + \exp(\beta_0 + \sum \beta_i \cdot LP_i)} \quad , \quad (\text{a-2})$$

where  $\beta_0$  is the intercept and  $\beta_i$  is the  $i$ -th coefficient of the logistic regression model.

These parameters can be estimated by SAS procedure, PROC LOGISTIC, using the method of maximum likelihood.

A set of logistic regression coefficients was computed based on the original lab data. In their investigation of bovine lameness, Liu *et al.* (2009) demonstrated that the accuracy of the predictions of such models is significantly improved when the  $LPs$  are transformed via B-spline transformations. An implementation of these transformations is available in SAS (PROC TRANSREG). We will refer to these as transformed locomotion parameters ( $TLPs$ ). The Leave-One-Out (LOO) method using B-spline cross validation was used to evaluate the performance of the model. See Efron and Tibshirani (1993) for further details about this method. For the SOD1-G93A experiment, Tang *et al.* (2009a) selected 7  $TLPs$  to build the SOD1-G93A model. The performance of models with increasing number (1, 3, 5, and 7) of  $TLPs$  was shown in Figure 3.1. The prediction performance improves as expected.

The logistic regression model and LOO technique has been successfully applied to two projects. Tang *et al.* (2009b) applied this to build a model (with 6  $TLPs$ ) for detecting gait differences induced by denervation, and Tang *et al.* (2010) built a

successful model for predicting lab induced Parkinson's disease based on gait impairment.

### **1.5. Obtaining the Dataset**

The source dataset for the sample size calculation described in this manuscript is from an experiment which measures early pre-symptomatic changes in locomotion of SOD1-G93A rats by Tang *et al.* (2009a).

The study comprises 4 SOD1-G93A and 4 Sprague-Dawley (SD) control rats from Taconic Laboratory (Germantown, NY). The 4 SOD1-G93A rats each had 11, 74, 58, and 31 repeated runs, respectively, and 4 control rats each had 5, 45, 38 and 16 repeated runs, respectively. The control group is considered normal while the corresponding gait abnormality is scored as 0 in the model; SOD1-G93A is the designated treatment group while the corresponding gait abnormality is scored as 1 in the model. The logistic model then provides a prediction equation based on the *TLPs*.

## **2. Sample Size Determination**

### **2.1. Prediction Accuracy**

The fundamental question of our analysis is, of course, to determine the number of rats needed for a viable experiment. Dobbin and Simon (2007) introduce a methodology for sample size determination for prediction in the context of high-dimensional data that captures variability in both steps of predictor development. In this paper, we will address this question in the context of GAS. The logistic regression model is the statistical model underlying the GAS technology employed here. Thus, the question of optimal sample size does not lend itself to an easy and closed solution. In fact, there are a number of choices in the objective function for

deriving the sample size. Since our primary objective is to develop a predictive model and to ascertain if the predictive ability of the model has a high accuracy, we will investigate the sample size issue from the aspect of efficient estimation of misclassification probability by cross validation. In order to classify subjects into binary groups, the receiver operating characteristic (ROC) curve is widely used for judging the discrimination ability of different statistical models by Liu and Wu (2008), and Faraggi and Reiser (2002). The ROC curve can be estimated by two approaches: parametric method and nonparametric method. See Zhao (2008) for details about these two methods. The logistic regression model is used to predict the probability of whether a specific subject belongs to a particular group by Hosmer and Lemeshaw (2000).

Meanwhile, several important, practical issues need to be considered. First, even though the rats are very expensive, running repeated measurements on each rat is relatively easy and inexpensive. Second, rats (divided into treatment group and a control group) will be monitored over several days during the clinical study in order to evaluate the efficacy of the treatment under consideration. Therefore, our approach to sample size determination will need to take both repeated and the longitudinal measurements issues into account.

We assume the *LPs* of each rat have a multivariate normal distribution with the parameters computed from the lab data mentioned above. The new simulated dataset is generated based on this assumption. Our approach to sample size determination is based on simulating data from the ALS model and examining the gains in terms of estimating the LOO correct classification rate.

## 2.2. Simulation Approach

Sample size determination for model building needs the choice of a statistic to measure the performance. In this case, we evaluate the performance of our models by the misclassification rates that are also obtained as the area under the ROC curve. Then we make the estimation on an optimal sample size, i.e. the number of rats and number of runs per rat, to estimate the misclassification probabilities with a high degree of accuracy. We also track the standard errors of the estimated coefficients of the logistic regression model as a function of the sample size.

Clearly, the current pilot study has too few rats, and we will need to collect data from a much larger group. There are several key elements to the sample size determination. The objective of our study is to come up with a predictive model of the form (1) which accurately predicts the gait abnormality.

In our simulation, we first calculated the means of the *LPs* in each case (control and SOD1-G93A) and the overall covariance matrices of the two groups based on the lab data. We derived the desired number of animals by: (i) stabilizing the classification rate, and (ii) stabilizing the standard errors of each of the logistic regression coefficients in the SOD1-G93A model.

In model building, we use the LOO estimates of misclassification rates as the criteria for determining the best model. For generating data, we postulate the following logistic regression model for the *j*th run of the *r*th rat. Let  $Y_{rj}=1$  if the *r*th rat showed ALS symptom during the *j*th run, and let

$$P(Y_{rj} = 1) = \pi_{rj} = \frac{\exp\left(\beta_0 + \sum_{i=1}^k \beta_i \cdot TLP_{irj}\right)}{1 + \exp\left(\beta_0 + \sum_{i=1}^k \beta_i \cdot TLP_{irj}\right)}, \quad (\text{a-3})$$



where  $k$  is the number of TLPs included in the model. We can incorporate the within and between rat variability into the model (a-3) in order to generate the simulation data:

$$\begin{pmatrix} TLP_{1rj} \\ \vdots \\ TLP_{krj} \end{pmatrix} = \begin{pmatrix} TLP_{1r} \\ \vdots \\ TLP_{kr} \end{pmatrix} + \begin{pmatrix} \eta_1 \\ \vdots \\ \eta_k \end{pmatrix}, \quad (\text{a-4})$$

where  $\eta_i$  is an independently and identically distributed multivariate normal random variable.

Following the hierarchical structure of model equations (a-3) and (a-4), we generate the *TLP* data in two steps. For a given value of the  $\beta$ -coefficients, we first generate the *TLP* average values corresponding to  $r$ th rat, and then further generate the *TLP* values corresponding to  $n_r$  runs of the  $r$ th rat. We use the mean and covariance statistics from the pilot data as the parameters of the multivariate normal distribution. This hierarchical approach enables us to incorporate the correlation between runs corresponding to the same rat. Our simulations are based on this model.

From the current data set, we compute the following statistics for the *TLPs*. Recall that  $TLP_{irj}$  denotes the  $i$ th *TLP* for the  $r$ th rat in the  $j$ th run. We include an additional subscript to denote whether or not a rat belongs to a control group or to the SOD1-G93A group. That is, we let  $TLPC_{irj}$  indicate the  $i$ th *TLP* for the  $r$ th rat, in the  $j$ th run, in the control group. Similarly,  $TLPD_{irj}$  denotes the  $i$ th *TLP* for the  $r$ th rat, in the  $j$ th run, in the disease group.

For the control group,

$$\mathbf{TLP}_{C\bullet\bullet} = \begin{pmatrix} TLP_{C1\bullet\bullet} \\ \vdots \\ TLP_{Ck\bullet\bullet} \end{pmatrix} \quad (\text{a-5})$$

is the vector means, where

$$TLP_{Ci\bullet\bullet} = \frac{1}{N-1} \sum_{r=1}^R \sum_{j=1}^{n_r} TLP_{Cirj} \quad , \quad (\text{a-6})$$

where  $N$  is the total number of runs, and

$$\hat{\Omega}_C = \frac{1}{N-1} \sum_{r=1}^R \sum_{j=1}^{n_r} (TLP_{Cirj} - \overline{TLP}_{Ci\bullet\bullet}) (TLP_{Cirj} - \overline{TLP}_{Ci\bullet\bullet})' \quad (\text{a-7})$$

Similarly, we can define for the disease group. Now, we can obtain the  $(u, v)^{th}$  element of the within rat variance and covariance matrix  $\hat{\Omega}_w$  as follows:

$$\hat{\Omega}_w(u, v) = \frac{1}{\sum_{r=1}^R (n_r - 1)} \sum_{r=1}^R \sum_{j=1}^{n_r} (TLP_{Curj} - \overline{TLP}_{Cur\bullet}) (TLP_{Cvrj} - \overline{TLP}_{Cvr\bullet})' \quad (\text{a-8})$$

The overall variance-covariance matrix  $\hat{\Omega}_c$  is used for generating the  $TLP$  values for the rats and  $\hat{\Omega}_w$  is used for generating the  $TLP$  values for various runs within each rat. In summary, we simulated the procedure in the following steps:

1. We generate a new simulated dataset with 10 rats per group (control and SOD1-G93A), and each rat has 20 repeated runs.
2. The logistic regression method is then applied to calculate the probabilities of a test run belonging to SOD1-G93A rats in this new simulated dataset, which has 400 observations (200 per group). The correct logistic regression classification rate based on SOD1-G93A model is recorded. The corresponding standard errors of the classification rates and the standard errors of the coefficients in the model for different numbers of rats are also tracked. The cutoff line for the classification was 0.5.

3. In order to reach a reliable simulation result, step 1 and 2 were then repeated 1000 times, which is both an arbitrary number and is also big enough. The average of classification rate is computed based on these 1000 simulated datasets.
4. Step 1, 2 and 3 is then repeated for 20, 30, 40, etc. rats per group. Then, the average of the classification rate and the corresponding standard errors, the maximum standard error of the  $\beta$ s in the logistic regression model, can be found for variant numbers of rats. One can make the decision on how many rats are going to be run according to the information given above.

### 3. Conclusion

We would expect to see an inverse relationship between the numbers of rats with the estimated classification rates. If there are fewer rats in the experiment, the logistic model will be more likely to cluster the similar data into their appropriated groups, i.e. high classification rate. On the other hand, if we recruit more rats into the experiment, then the failure to cluster the corrected group will be high, i.e. a higher misclassification rate. However, the classification rate will approach the true population parameter as the number of rats becomes larger. Therefore, it would be reasonable to select the number of rats at which the classification rate begins to stabilize with an acceptable degree of accuracy.

Figure 6.1 demonstrates that the classification rate decreases as the number of animals per group increases from 10 to 200. The standard deviation of the classification rate is presented by the vertical bars. One can observe that the classification rate approaches 0.86; the standard deviation decreases as the number of

animals increases. Nevertheless, when the number of animals per group is about 50, the classification rate will have already reached a reasonably stable stage.

As anticipated, the curve is a decreasing function of the number of rats in Figure 6.1. The standard deviation of each classification rate is also included into the plot. We noticed that standard deviation bars are getting narrower as the number of rats increases. The classification rate converges as the number of rats increases. Most importantly, we see that the classification rate also reaches the stable level between 50 to 60 rats. The curve does not fluctuate beyond 50 or 60 rats; hence, we believe that 50 rats per group will be an adequate sample size.

Figure 6.2 depicts the maximum standard deviation of the coefficients of the logistic regression model divided by the values of the maximum logistic regression coefficient. This standard error is plotted versus number of rats per group. This plot indicates that the maximum standard error is low and stable when the number of rats in each group is 20. We therefore decided to test 50 SOD1-G93A and 50 control SD rats in the future ALS experiment.

Furthermore, another approach to check the sample size could be the stabilization of logistic regression coefficients. In step 2 of the simulation, we also output the standard error of the logistic regression coefficients. At the completion of step 3, we will get 1000 sets of standard errors for each of logistic regression coefficients in SOD1-G93A model.

The average standard errors of each coefficient are computed based on these 1000 iterations. We then used the SOD1-G93A model to compute the logistic regression coefficients on the transformed data and to divide them into the average standard

errors in order to standardize the averages. The maximum output of the 28 ratios is kept as the upper threshold of the coefficient variability. Step 4 is then repeated for the different number of rats. Figure 6.2 showed that the maximum standard error of the logistic regression coefficients started to stabilize around 40 or 50 rats. This result confirmed that 50 rats is a reasonable sample size.

#### **4. Discussion**

An efficient design is very important for running experiments involving animals primarily because it can reduce the cost of these experiments. In this manuscript, we simulate the sample sizes for the gait analysis experiment of laboratory rats by using the data we gathered. The average of classification rates and the maximum standard error of the coefficients in the logistic regression model versus the number of animals in each group are plotted. The sample size of the experiment can be therefore determined by the plots.

The area under the ROC curve is usually used as a measure for the effectiveness of diagnostic markers. In this paper, we use ROC to evaluate the performance of the models. It is also proved that the number of runs from one rat is not significantly related to the classification rates.

#### **5. Acknowledgements**

The financial support provided by the Laboratory of Neurosciences at NIA and the technical support of Dr. Donald K. Ingram are gratefully acknowledged. Support was also provided by the Veterans Administration (PY). Furthermore, the support of the staff of the animal facility at UMBC, Ms. Kirsty L. Carrihill-Knoll and Ms. Rosie Mills, is greatly appreciated.

## Bibliography

- [1]. Amende I, Kale A, McCue S, Glazier S, Morgan JP, Hampton TG. *Gait dynamics in mouse models of Parkinson's disease and Huntington's disease*. J Neuroeng. Rehab, 2005; 2:1743–1768.
- [2]. Andlin-Sobocki P, Jonsson B, Wittchen H-U, Olesen J. *Cost of disorders of the brain in Europe*. European J. of Neurology, 2005; 12 (1): 1-27.
- [3]. Babu GN, Kumar A, Chandra R, Puri SK, Singh RL, Kalita J, Misra UK. *Oxidant-antioxidant imbalance in the erythrocytes of sporadic amyotrophic lateral sclerosis patients correlates with the progression of disease*. Neurochemistry International, 2008; 52: 1284-1289.
- [4]. Berryman ER, Harris RL, Moalli M, Bagi CM. *Digigait™ quantitation of gait dynamics in rat rheumatoid arthritis model*. J. Musculoskelet Neuronal Interact, 2009; 9(2):89-98.
- [5]. Best TM. *Soft-tissue injuries and muscle tears*. Clinics in Sports Medicine, 1997; 16: 419-434.
- [6]. Bozkurt A, Deumens R, Scheffel J, O'Dey DM, Weis J, Joosten EA, Fuhrmann T, Brook GA, Pallua N. *CatWalk gait analysis in assessment of functional recovery after sciatic nerve injury*. J. of Neuroscience Methods, 2008; 173: 91-98.
- [7]. Brault JR, Siegmund GP, Wheeler JB. *Cervical muscle response during whiplash: evidence of a lengthening muscle contraction*. Clinical Biomechanics, 2000; 15: 426-435.
- [8]. Cheng H, Almstrom S, Gimenez-Llort L, Chang R, Ogren SO, Hoffer B, Olson L. *Gait analysis of adult paraplegic rats after spinal cord repair*. Exp Neurol, 1997; 148(2): 544-557.
- [9]. Clarke KA. *Swing time changes contribute to stride time adjustment in the walking rat*. Physio Behav 1991; 50(6):1261–1262.
- [10]. DelloRusso C, Crawford RW, Chamberlain JS, Brooks SV. *Tibialis anterior muscles in mdx mice are highly susceptible to contraction-induced injury*. J Muscle Res Cell Motil 2001; 22: 467–475.
- [11]. Deumens R, Jaken RJP, Marcus MAE, Joosten EAJ. *The CatWalk gait analysis in assessment of both dynamic and static gait changes after adult rat sciatic nerve resection*. J. of Neuroscience Methods, 2007; 164: 120-130.
- [12]. Dobbin KK, Simon RM. *Sample size planning for developing classifiers using high dimensional DNA microarray data*. Biostatistics, 2007; 8: 101-117.

- [13]. Durbeej M, Campbell KP. *Muscular dystrophies involving the dystrophinglycoprotein complex: an overview of current mouse models*. *Curr Opin Genet Dev*, 2002; 12: 349–361.
- [14]. Efron B, Tibshirani RJ. *An introduction to the bootstrap*. New York: Chapman & Hall; 1993.
- [15]. Fagotti A, Gabbiani G, Pascolini R, Neuville P. *Multiple isoform recovery (MIR)-PCR: a simple method for the isolation of related mRNA isoforms*. *Nucleic Acids Research*, 1998; 26: 2031-2033.
- [16]. Faraggi D, Reiser B. *Estimation of the area under the ROC curve*. *Statistics in Medicine*, 2002; 21: 3093-3106.
- [17]. Feng X, Tang W, Tasch U, Neerchal N. *Designing a Study for Developing Predictive Models for Gait Abnormality in Rat*. *J. of Statistical Computation and Simulation*, under review.
- [18]. Fischer LR, Culver DG, Tennant P, Davis AA, Wang M, Casteelano-Sanchez A, Khan J, Polak MA, Glass JD. *Amyotrophic lateral sclerosis is a distal axonopathy: evidence in mice and man*. *Experimental Neurology*, 2004; 185: 232-240.
- [19]. Full RJ, Tu MS. *Mechanics of six-legged runners*. *Journal of Experimental Biology*, 1990; 148: 129-146.
- [20]. Gabriel AF, Marcus MAE, Honig WMM, Walenkamp GHIM, Joosten EAJ. *The CatWalk method: A detailed analysis of behavioral changes after acute inflammarty pain in the rat*. *J. of Neuroscience Methods*, 2007; 163: 9-16.
- [21]. Galán L, Vela A, Guerrero A, Barcia JA, García-Verdugo JM, Matias-Guiu J. *Experimental models of amyotrophic lateral sclerosis*. *J. of Neurologia*, 2007; 22(6): 381-388.
- [22]. Garbuzova-Davis S, Willing A E, Milliken M, Saporta S, Sowerby B, Cahill D W, Sanberg P R. *Intraspinal implantation of hNT neurons into SOD1 mice with apparent motor deficit*. *ALS and Other Motor Neuron Disorders*, 2001; 2: 175-180.
- [23]. Garrett Jr. WE. *Muscle strain injuries*. *American J. of Sports Medicine*, 1996; 24: S2-S8.
- [24]. Guillot TS, Asress SA, Richardson JR, Glass JD, Miller GW. *Treadmill gait analysis does not detect motor deficits in animal*. *J. of Motor Behavior*, 2008; 40: 568-577.
- [25]. Guvot MC, Hantraye P, Dolan R, Palfi S, Maziere M, Brouillet E.

*Quantifiable bradykininemia, gait abnormalities and Huntington's disease-like striatal lesions in rats chronically treated with 3-nitropropionic acid.* Neuroscience, 1979; 79(1): 45–46.

[26]. Hamer PW, McGeachie JM, Davies MJ, Grounds MD. *Evans Blue Dye as an in vivo marker of myofibre damage: optimising parameters for detecting initial myofibre membrane permeability.* J Anat, 2002; 200: 69–79.

[27]. Hamers FPT, Lankhorst AJ, Van Laar TJ, Veldhuis WB, Gispen WH. *Automated quantitative gait analysis during overground locomotion in the rat: its application to spinal cord contusion and transaction injuries.* J. of Neurotrauma, 2001; 18: 187-201.

[28]. Hampton TG, Stasko MR, Kale A, Amende I, Costa ACS. *Gait dynamics in trisomic mice: quantitative neurological traits of Down syndrome.* Physiology & Behavior, 2004; 82(2-3): 381-389.

[29]. Hjorth JSU. *Computer intensive statistical methods—validation model selection and bootstrap.* London: Chapman & Hall; 1994.

[30]. Howland DS, Liu J, She Y, Goad B, Maragakis NJ, Kim B, et al. *Focal loss of the glutamate transporter EAAT2 in a transgenic rat model of SOD1 mutant-mediated amyotrophic lateral sclerosis (ALS).* Proc Natl Acad Sci, 2002; 99(3):1604–1609.

[31]. Hosmer DW, Lemeshaw S. *Applied Logistic Regression.* John Wiley and Sons, Inc: New York, 2000.

[32]. Jackson M, Ganel R, Rothstein JD. *Models of amyotrophic lateral sclerosis.* Curr Protoc Neurosci, 2002; 9: Unit 9.13.

[33]. Kafkafi N, Yekutieli D, Yarowsky P, Elmer GI. *Datamining in a behavioral test detects early symptoms in a model of amyotrophic lateral sclerosis.* Behav Neurosci, 2008; 122: 777–787.

[34]. Keny CS. *Developing new technologies for detecting lameness in equines.* Master's thesis. UMBC, 2005.

[35]. Kettler A, Hartwig E, Schultheiss M, Claes L, Wilke HJ. *Mechanically simulated muscle forces strongly stabilize intact and injured upper cervical spine specimens.* J. of Biomechanics, 2002; 35: 339-346.

[36]. Koopmans GC, Brans M, Gomez-Pinilla F, Duis S, Gispen WH, Torres-Aleman I, Joosten EAJ, Hamers FPT. *Circulating insulin-like growth factor I and functional recovery from spinal cord injury under enriched housing conditions.* European Journal of Neuroscience, 2006; 23: 1035-1046.



[37]. Kopf A, Pawelka S, Kranzl A. *Clinical gait analysis--methods, limitations and possible applications*. Acta Med Austriaca, 1998; 25(1): 27-32.

[38]. Li S, Kim JE, Budel S, Hampton TG, Strittmatter SM. *Transgenic inhibition of Nogo-66 receptor function allows axonal sprouting and improved locomotion after spinal injury*. Molecular and Cellular Neuroscience, 2005; 29: 26-39.

[39] Li S, Ji-Eun Kim, Budel, S, Hampton, T. G., Strittmatter, S. M.. *Transgenic inhibition of Nogo-66 receptor function allows axonal sprouting and improved locomotion after spinal injury*, Molecular and Cellular Neuroscience, 2005; 29: 26-39.

[40]. Liao F, Wang J, He P. *Multi-resolution entropy analysis of gait symmetry in neurological degenerative diseases and amyotrophic lateral sclerosis*. Medical Engineering & Physics, 2008; 30: 299-310.

[41]. Lin K-L, Yang D-Y, Chu I-M, Cheng F-C, Chen C-J, Ho S-P, Pan H-C. *DuraSeal as a ligature in the Anastomosis of rat sciatic nerve gap injury*. J. of Surgical Research, 2010; 161: 101-110.

[42]. Liu J, Dyer RM, Neerchal NK, Rajkondawar PG, Tasch U. *Enhancing the predictions accuracy of Bovine Lameness Models through Nonlinear Transformations of the Limb Movement Variables*. 15<sup>th</sup> International Symposium on Lameness in Ruminants. Koupio, Finland, 2008.

[43]. Liu J, Neerchal NK, Tasch U, Dyer RM, Rajkondawar PG. *Enhancing the predictions accuracy of bovine lameness models through nonlinear transformations of the limb movement variables*. J Dairy Sci., 2009; 92: 2539–2550.

[44]. Liu H, Wu T. *Estimating the Area under a Receiver Operating Characteristic (ROC) Curve for Repeated Measures Design*. J. Statistical Software, 2008; i12.

[45]. Lovering RM, Roche JA, Bloch RJ, De Deyne PG. *Recovery of function in skeletal muscle following 2 different contraction-induced injuries*. Arch Phys Med Rehabil, 2007; 88: 617-625.

[46]. Lovering RM, Hakim M, Moorman III CT, De Deyne PG. *The contribution of contractile pre-activation to loss of function after a single lengthening contraction*. J. of Biomechanics, 2005; 38: 1501-1507.

[47]. Mak MKY, Patla A, Hui-Chan C. *Sudden turn during walking is impaired in people with Parkinson's disease*. Exp Brain Res, 2008; 190: 43–59.

[48]. Matsumoto A, Okada Y, Nakamichi M, Nakamura M, Toyama Y, Sobue G, Nagai M, Aoki M, Itoyama Y, Okano, H. *Disease progression of human SOD1 (G93A) transgenic ALS Model rats*. J. of Neuroscience Research, 2006; 83: 119-133.

[49]. Metz GA, Tse A, Ballermann M, Smith LK, Fouad K. *The unilateral 6-OHDA rat model of Parkinson's disease revisited: an electromyographic and behavioural analysis*. Eur. J. Neurosci., 2005; 22:735–744.

[50]. Miklyaeva EI, Casteneda E, Whishaw IQ. *Skilled reaching deficits in unilateral dopamine-depleted rats: impairments in movement and posture and compensatory adjustments*. J Neurosci, 1994; 14: 7148–7158.

[51]. Moubarak, P., *Design of a Novel Gait Analysis System Measuring 3-D Ground Reaction Forces in Rodents for Biomedical and Pharmaceutical Research Applications*. Master's thesis. UMBC, 2007.

[52]. Muir GD, Whishaw IQ. *Ground reaction forces in locomoting hemiparkinsonian rats: a definitive test for impairments and compensations*. Exp Brain Res, 1999; 126: 307-314.

[53]. Muir GD, Whishaw IQ. *Complete locomotor recovery following corticospinal tract lesions: measurement of ground reaction forces during overground locomotion in rats*. Behav Brain Res, 1999; 103(1): 45–53.

[54]. Neerchal NK, Tasch U. *Enhancing model prediction accuracy by using spline transformations*. Pending patent application; 2008.

[55]. Neumann M, Wang Y, Kim S, Hong SM, Jeng L, Bilgen M, Liu J. *Assessing gait impairment following experimental traumatic brain injury in mice*. J. of Neuroscience Methods, 2009; 176: 34-44.

[56]. Nicaise C, Coupier J, Dabadie MP, Decker RD, Mangas A, Bodet D, Poncelet L, Geffard M, Pochet R. *Gemals, a new drug candidate, extends lifespan and improves electromyographic parameters in a rat model of amyotrophic lateral sclerosis*. Amyotrophic Lateral Sclerosis, 2008; 9: 85-90.

[57]. Niebroj-Dobosz I, Rafałowska J, Fidziańska A, Gadamski R, Grieb P., *Myelin composition of spinal cord in a model of amyotrophic lateral sclerosis (ALS) in SOD1G93A transgenic rats*. Folia Neuropathologica, 2007; 45(4): 236-241.

[58]. Niu Q, Yang Y, Zhang Q, Niu P, He S, Di Gioacchino M, Conti P, Boscolo P., *The relationship between Bcl-gene expression and learning and memory impairment in chronic aluminum-exposed rats*. J. of Neurotoxicity research, 2007; 12(3): 163-169.

[59]. Noldus Information Technology, 2006. <[http://74.125.95.132/search?q=cache:nmQmyEBse-EJ:www.trendconsortium.nl/file\\_download/7+CatWalk+Noldus&hl=en&ct=clnk&cd=4&gl=us.](http://74.125.95.132/search?q=cache:nmQmyEBse-EJ:www.trendconsortium.nl/file_download/7+CatWalk+Noldus&hl=en&ct=clnk&cd=4&gl=us.)>

[60]. Offen D, Barhum Y, Melamed E, Embacher N, Schindler C, Ransmayr G. *Spinal Cord mRNA profile in patients with ALS: Comparison with transgenic mice expressing the human SOD-1 Mutant*. J. Mol Neurosci, 2009; 38: 85-93.

[61]. Plotnik M, Giladi N, Hausdorff J. *Bilateral coordination of walking and freezing of gait in Parkinson's disease*. Eur. J Neurosci, 2008; 27: 1999–2006.

[62]. Rajkondawar PG, Tasch U, Lefcourt AM, Erez B, Dyer RM, Varner MA. *A system for identifying lameness in dairy cattle*. Applied Engineering in Agriculture, 2001; 18: 87-96.

[63]. Rajkondawar PG, Lefcourt AM, Neerchal NK, Dyer RM, Varner MA, Erez B, Tasch U. *The development of an objective lameness scoring system for dairy herds: pilot study*. Trans ASAE, 2002; 45: 1123–1125.

[64]. SAS Institute, Inc., 2004. SAS/STAT 9.1 User's Guide. Cary, NC.

[65]. Schober A. *Classic toxin-induced animal models of Parkinson's disease: 6-OHDA and MPTP*. Cell Tissue Res, 2004; 318: 215-224.

[66]. Schumaker LL. *Spline functions: basic theory*. 3rd ed. Cambridge, UK: Cambridge University Press; 2007.

[67]. Steele JC, McGeer PL . *The ALS/PDC syndrome of Guam and the cycad hypothesis*. Neurology, 2008; 70: 1984-1990.

[68]. Suzuki M, Tork C, Shelley B, McHugh J, Wallace K, Klein SM, Lindstrom MJ, Svendsen CN. *Sexual dimorphism in disease onset and progression of a rat model of ALS*. J. of Amyotrophic Lateral Sclerosis, 2007; 8(1): 20-25.

[69]. Tang W, Tasch U, Neerchal NK, Zhu L, Yarowsky, P. *Measuring early pre-symptomatic changes in locomotion of SOD1-G93A rats – a rodent model of Amyotrophic Lateral Sclerosis*. J. Neurosci. Methods, 2009a; 176(2): 254-62.

[70]. Tang W, Lovering RM, Roche JA, Bloch RJ, Neerchal NK, Tasch U. *Gait analysis of locomotory impairment in rats before and after neuromuscular injury*. J. Neurosci. Methods, 2009b; 181(2): 249-56.

[71]. Tang W, McDowell K, Limsam M, Neerchal KN, Yarowsky P, Tasch U. *Locomotion analysis of Sprague-Dawley rats before and after injecting 6-OHDA*. Behavioral Brain Research, 2010, 210:131-133.

[72]. Tasch U, Moubarak P, Tang W, Zhu L, Lovering RM, Roche J, Bloch RJ. *An instrument that simultaneously measures spatial gait parameters and ground reaction forces of locomoting rats*. Proceedings of the 9<sup>th</sup> Biennial ASME Conference on Engineering Systems Design and Analysis. ESDA08. July 7-9. Haifa, Israel, 2008.

[73]. Thonhoff JR, Jorda PM, Karam JR, Bassett BL, Wu P. *Identification of early disease progression in an ALS rat model*. Neuroscience letters, 2007; 415: 264-268.

[74]. Twelves D, Perkins KS, Counsell C. *Systematic review of incidence studies of Parkinson's disease*. Mov Disord, 2003; 18: 19-31.

[75]. Walker JL, Evans JM, Meade P, Resig P, Siskin BF. *Gait-stance duration as a measure of injury and recovery in the rat sciatic nerve model*. J. Neurosci Methods, 1994; 52(1): 47-52.

[76]. Wooley CM, Sher RB, Kale A, Frankel WN, Cox GA, Seburn KL. *Gait analysis detects early changes in transgenic SOD1 (G93A) mice*. Muscle Nerve, 2005; 32: 43-50.

[77] Zhao Z. *Parametric and nonparametric models and methods in financial econometrics*. Statistics Surveys, 2008; 2, DOI: 10.1214/08-SS034.

